THE PENNSYLVANIA STATE UNIVERSITY
SCHREYER HONORS COLLEGE

DEPARTMENT OF NUTRITIONAL SCIENCES

A COMPARISON OF *STREPTOCOCCUS PNEUMONIAE SEROTYPE 3 AND SEROTYPE 14 INFECTION IN NEONATAL MICE*

TIFFANY BERNARDO
SPRING 2014

A thesis
submitted in partial fulfillment
of the requirements
for a baccalaureate degree
in Nutritional Sciences
with honors in Nutritional Sciences

Reviewed and approved* by the following:

A. Catharine Ross, Ph.D.
Professor of Nutritional Sciences and Occupant of the Dorothy Foehr Huck Chair
Thesis Supervisor

Rebecca Corwin, Ph.D., RD
Professor of Nutritional Neuroscience
Honors Adviser

* Signatures are on file in the Schreyer Honors College.

ABSTRACT

Streptococcus pneumoniae, commonly referred to as the pneumococcus, is a Gram positive pathogen that colonizes the upper airways of humans (1). *S. pneumoniae* is the most frequent cause of community-acquired pneumonia, which occurs when the pneumococcus populates the lower bronchi, and is often the cause of otitis media in children (1, 2). This bacterium is also responsible for certain invasive diseases, such as sepsis and meningitis (3). *S. pneumoniae* colonization, pathogenesis, and clearance is well−documented in adults, but very few papers have characterized the effect of *S. pneumoniae* infection in neonates. Thus, the goal of the present study was to develop a model of pneumococcal disease in neonatal mice, and determine the efficacy of vitamin A (VA) supplementation on *Streptococcus pneumoniae*−induced pneumonia pathogenesis.

Streptococcus pneumoniae serotype 3 (ST3) and serotype 14 (ST14) were chosen as a model of invasive and localized pneumococcal infection, respectively. We found that ST14 infection causes a large neutrophil influx to the lung 24 and 48 hours post−infection, while ST3 causes very little granulocyte migration. A myeloperoxidase (MPO) assay was used to confirm the increased levels of neutrophil activity during an acute infection with ST14. Furthermore, VA supplementation was found to have no effect on lung colonization, bacterial migration, or cellular infiltration, but VA supplementation significantly increased liver retinol levels. The data gathered in this study can be used to further knowledge regarding the complex interaction between diet, the host immune system, and bacterial pathogenesis.

TABLE OF CONTENTS

LIST OF FIGURES

LIST OF TABLES

Chapter 1

Background

Introduction to *Streptococcus pneumoniae*–induced Pneumonia

Streptococcus pneumoniae, commonly referred to as the pneumococcus, is a major respiratory pathogen that colonizes the upper airways of humans (1). *S. pneumoniae* is the most frequent cause of community-acquired pneumonia, which occurs when the pneumococcus populates the lower bronchi, and is often the culprit of otitis media in children (1, 2). This bacterium is also responsible for certain invasive diseases, such as sepsis and meningitis (3). Although the pneumococcus is a commensal pathogen, it must express abnormally virulent traits in order to maintain life inside the competitive atmosphere of the nasopharynx, where it colonizes the mucosal surface (2, 3). Once the bacterium spreads from the nasal mucosal surface onto other more inferior portions of the airways, a disease state has occurred; thus a logical first step in *S. pneumoniae* pathogenesis is colonization (4). This first step is more conventionally cited as the carrier state, where no clinical manifestations of disease are apparent. It is widely accepted that the carrier state has large implications in innate and adaptive immunity of the host, which will further be explored in this review. This review will also examine the microbiology of *S. pneumoniae*, pathogenicity, mortality and morbidity, clinical features, and also immunization and research advances in the treatment and prevention of *S. pneumoniae.*

Structure

Streptococcus pneumoniae is a Gram-positive cocci-shaped bacterium of the genus *Streptococcus* (2). *S. pneumoniae* is alpha-hemolytic, meaning that it has the ability to partially lyse red blood cells, and is highly pathogenic (5). *S. pneumoniae* contains a large amount of peptidoglycan

(PEPTG) in its cell wall, and does not contain an outer membrane. PEPTG is a highly organized polymer of amino sugars that, when linked together in what is known as a crystal lattice structure, compose the cell wall of Gram positive bacteria. This cross-linking provides enormous amounts of strength and structure to the cell wall. The outer layer of the bacterial cell wall, the capsule, is also implicated in identification of the various serotypes; that is, each individual serotype (ST) contains a specific mixture of polysaccharides that is identifiable and unique (6, 7). The capsule is a highly organized polysaccharide polymer that is covalently attached to cell wall PEPTG. There are at least ninety different serotypes of *S. pneumoniae* that have been characterized thus far (2). Apart from providing serotype information, the capsule also contains numerous traits that make it especially virulent, such as the ability to evade phagocytosis and clearance by innate immune mechanisms within the respiratory system (7, 8). Finally, the capsule also has the ability to undergo phase variation (2). The pneumococcus initially displays a thick capsule that can inhibit the bacterium in attaching to host cells (2). To overcome this problem, *S. pneumoniae* will undergo phase variation. Phase variation is the process in which a bacterium will switch its phenotype; in the case of the pneumococcus, this organism undergoes phase variation from a transparent to an opaque capsule. Adhesins, in addition to a few other proposed molecules, that are located in the cell wall are associated with the pathogen-epithelial cell interaction (2). When the pneumococcus is attempting to bind to the host's epithelial cell, the bacterium will display a transparent phenotype that does not interfere with the binding interaction, and also helps the bacterium attach (2). Opsonophagocytic killing is much more apparent once the bacterium beings to migrate into more sterile areas such as the terminal bronchi or the bloodstream, thus the pneumococcus will switch to the opaque capsule phenotype, which is more resistant to phagocytic action (2). Additionally, the capsule defends the pneumococcus during the innate inflammatory response when neutrophils have been attracted to the area (9). Adding to the bacterium's virulence is the exotoxin pneumolysin, which is a member of the cholesterol-

dependent cytolysin family (10). When secreted by *S. pneumoniae*, pneumolysin has the ability to puncture pores into the host's cells, causing it to lyse due to osmotic pressures (8). Interestingly, non−encapsulated bacterial strains are not known to cause disease (11).

After culturing and isolating bacteria from throat swab, nose swab, sputum, or other more uncommon body fluids such as blood or cerebrospinal fluid, the bacteria can be grown on blood agar plates at 37°C in a CO_2 incubator (5, 8). Since *S. pneumoniae* is a member of the viridians family, a term commonly used to refer to species in the *Streptococcus* family capable of alpha-hemolysis, a green-brown pigment will be observed on the agar where the red blood cells were partially lysed (5). The colonies will appear round with well-defined edges, and a complete ring of alpha -hemolysis will surround the colony (5). The thick capsule will be visible on the plate, contributing a mucoid-like appearance to the colony. Once the bacterium has been Gram stained, it will appear a crystal violet color due to the large amount of peptidoglycan in their cell wall.

Serotypes

There are over ninety known serotypes (ST) of *S. pneumoniae*, but this review will focus on ST3 and ST14, which are commonly used in murine models of invasive and non−invasive pneumococcal pneumonia infection, respectively. ST3 has a large propensity to cause disease in both human and animals models, while ST14 causes a localized lung infection and can typically be cleared from the host without negative outcomes (i.e., meningitis, necrotizing pneumonia, and septic shock) (11). These differences are largely due to differences in capsule structure and thickness.

For example, the capsule surrounding ST14 consists of biosynthetic repeating tetrasaccharide units of 6)-[β-d-Gal*p*-(1→4)-]β-d-Glc*p*NAc-(1→3)-β-d-Gal*p*-(1→4)-β-d-Glc*p*-(1→}$_n$ (Pn14PS) (12). Class−switched IgG antibodies specific to each pneumococcal ST are most effective at clearing a pneumococcal pneumonia infection. A small organic molecule, Gal−Glc−(Gal−)GlcNAc, was found to be a particularly immunogenic epitope of *S. pneumoniae*

ST 14's capsule (12). Specifically, the small epitope was capable of inducing class−switched IgG antibodies specific to Pn14PS (12). Typically, bacteria that are encased in a capsule have the ability to evade the host immune response and roam undetected by immune cells. If detected, they normally only induce low−specificity IgM antibodies, which are much less effective in host defense (13). Thus, ST14 is rapidly cleared from the host, and negative outcomes are avoided.

Conversely, *S. pneumoniae* ST3 is encased in an immuno−evasive capsule that promotes sepsis and necrotizing pneumonia (11). *S. pneumoniae* ST3 is known for its thick, mucoid capsule that allows the bacterium to evade the host immune response. Lipsitch, et. al. (14) hypothesize that the bacterium is able to synthesize such a unique capsule because the repeating units that comprise the protective coating do not take a lot of energy to produce (14). Since ST3 has a thick capsule, the bacterium is able to avoid phagocytic uptake, allowing it to migrate from the lung to the bloodstream resulting in sepsis (11). Typically, ST3 generates a low antibody response, but a strong antibody response is generated in infants (14). However, the cause of this phenomenon is unknown.

Although a lot of information is known regarding capsule structure and biosynthesis, very little research has demonstrated the differences in serotype pathogenesis in neonates. Since *S. pneumoniae* infections are often found in children and elderly populations, we thought it was highly relevant to elucidate the similarities and differences in pathogenesis during an acute pneumococcal pneumonia infection. ST3 was chosen as a model of invasive pneumococcal disease, while ST14 was used to model a localized *S. pneumoniae* infection.

Pathogenesis

Streptococcus pneumoniae is transferred by direct contact with body fluids, such as sputum, of an infected individual (2). Once an individual has come in contact with the pneumococcus, the bacterium will take up residence on the mucosal surface of the individual's nasopharynx (6). If *S. pneumoniae* stays in the nasopharynx the individual will be asymptomatic, which is also known

as the carrier state (2, 15). However, the bacterium can move into uninfected areas of the host and cause numerous complications (4). Thus, colonization is necessary to precede infection, which typically occurs in early childhood (2, 4). Since children are the primary carriers of this pathogen, vaccination in early childhood is essential in reducing the pool of this pathogen, thus children under two years of age are now immunized with the seven valent conjugate vaccine, which is T cell dependent (8). This vaccine contains the seven most prevalent serotypes in the developed world (8). The pneumococcal capsular polysaccharide vaccine has also been very effective in preventing invasive pneumococcal disease, which contains twenty-three common pneumococcal serotypes (2, 8). Although this vaccine has contributed to mass amounts of herd immunity amongst non-vaccinated children, serotypes that were not prevalent in the developed world are now becoming more apparent because serotype-specific antibodies are developed by the host (2, 4, 8).

In a murine model of infection, a signaling cascade has been observed that brings an invasion of neutrophils to the area after inoculation with the pathogen, constituting part of the innate immune response (3). The pneumococcus proceeds to the respiratory and olfactory epithelium after inoculation, which results in recognition by the host and activation of the innate immune system (3, 6). The pneumococcus is first detected in the glycocalyx attempting to attach to the mucosal surface of the nasopharynx, where the transparent phenotype is expressed (2). The innate arm of the immune system will employ pattern recognition receptors such as the Toll-like receptors (TLRs), NOD-like receptors, RIG-I-like receptors, and DNA sensors located in the cytosol to detect the invading pathogen (6). These signaling events promote opening of the epithelial junctions, which allows for the influx of inflammatory mediators into the site of attachment (3). Activation of these receptors and sensors by molecules on the pathogen and on certain bacterial virulence traits results in the production of inflammatory mediators, which then recruit neutrophils to the infected area and activate the acute phase response (6). In one to three

days after colonization there is an influx of neutrophils to the designated area, which is also characterized as the primary infection (2,3). The molecular adhesion β2-integrin was once though to be essential in the influx of neutrophils to the infected area, but β2-integrin $^{-/-}$ mice showed normal neutrophil trafficking (8). Numerous adhesions have been implicated in the pathogenesis of *S. pneumoniae*, but mice lacking the adhesion molecule galectin-3 experience faster lung infiltration and early systemic dissemination of the pneumococcus (8). Galectin-3 is also involved in neutrophil recruitment, sending a signal to traffic neutrophils to the site of colonization (8). Furthermore, this adhesion molecule enhances pneumococci phagocytosis (8). Because pneumococci possess an opaque, thick capsule after they have attached to the mucosal surface, the bacterium is very resistant to phagocytosis by the invasive neutrophils (2, 15). The pneumococci will persist after the invasion of neutrophils has cleared (2, 3). If *S. pneumoniae* lacks the exotoxin pneumolysin, the influx of neutrophils will not be as robust and the carrier state will persist for a longer period of time in the host (3).

In order for the host's cells to attack the invading pathogen, serotype-specific antibodies are formed as well as complement proteins to augment phagocytosis (2). Although, the effectiveness of the humoral immune response must be paired with the inflammatory response and the cellular immune response to mount an effective immune response against *S. pneumoniae* (2). TLR2 is located on the plasma membrane of host cells and recognizes lipoteichoic acid and lipoproteins, both of which augment the inflammatory response (2, 6). Pneumococcal-specific IL-17 is initiated through TLR2, and also expresses $CD4^+$ T cells (15). In turn, macrophages and neutrophils are recruited to the area of infection and carriage is reduced (16). TLR2-/- mice showed reduced pneumococcal clearance during the later stages of colonization (2, 6). Furthermore, an important role for $CD4^+$ T cells, as opposed to humoral immunity, is showcased in major histocompatibility (MHC) class II $^{-/-}$ mice. Mice that do not express MHC class II also show an increased length of carriage, pointing towards the importance of the cellular immune

response (2). The acquisition of these natural $CD4^+$ T cells may lead to acquired immunity (16). Invasive pneumococcal disease occurs if the pathogen evades the initial host immune response and transits into the terminal bronchi (2, 4, 8). In the lower bronchial regions, where pneumococcal pneumonia is localized, the actions of cilia and mechanical mechanisms are not effective in clearance of the bacterium (17). Thus, the alveolar surface must employ different mechanisms to cleanse itself, or pneumococcal invasion can result in severe systemic infection or possibly death.

Clinical Features

As with other respiratory tract invasions, the onset of colonization by *S. pneumoniae* will evoke a mild upper airway aggravation (8). At the beginning of colonization the innate immune system and other respiratory defenses, such as the mucociliary escalator, antimicrobial peptides, and mechanical clearance (cough), will activate to clear the pathogen (8). If these systems should fail to rid the host of the pneumococci, the bacteria will travel to the lower bronchi and manifest as acute community-acquired pneumonia (8). The onset of community-acquired pneumonia is rapid, and the patient will present with a fever, cough (which can contain blood in the sputum), shaking chill, shortness of breath, and general discomfort (8). Chest pain is present in the majority of patients with community-acquired pneumonia (8). Treatment is available to patients, but if the bacterium is allowed to grow uncontrolled in the host the disease can progress to multiorgan failure, respiratory distress, bacteria actively dividing in the bloodstream (septicemia), and death (8). Upon examination of a radiograph in a patient presenting with pneumococcal pneumonia, one will see a progressively cloudy area in the lung where the bacterium has infiltrated (8). Due to the bacterium's ability to invade the bloodstream, heart, and brain, patients may first present with symptoms of sepsis, endocarditis, or meningitis before presenting with symptoms of pneumococcal pneumonia, therefore this disease can be difficult to diagnose (8). This problem is more common in severly immunocompromised patients, the very young or the

elderly, and in patients that develop pneumococcal pneumonia as a secondary infection (8). Finally, patients with asplenia and functional asplenia, both of which are forms of immunodeficiency, are at a greater risk of developing invasive pneumococcal disease and a higher mortality rate associated with the disease (18, 19).

Diagnosis of Pneumococcal Pneumonia

Streptococcus pneumoniae can be grown on blood agar plates at 37°C in a CO_2 incubator (5, 8). The bacterium adopts a crystal violet color when the Gram stain technique is employed (5). Also, due to the alpha hemolytic properties of *S. pneumoniae*, a distinct green – brown ring around the bacterial colonies will be easily identifiable (5, 8). Bacterial cultures can be obtained from sputum, blood, or other body fluids such as cerebrospinal fluid or urine (5, 8, 18). Catalase or optochin sensitivity assays are other methods useful in the identification of *S. pneumoniae* (19). The pneumococcus is catalase negative and optochin sensitive, further aiding in its identification (19).

The urinary antigen technique is a relatively new assay and is detected by immunochromatography (8). This assay detects the C polysaccharide in the patient's urine, which is located in the cell wall of the pneumococcus (8). Although this assay is noninvasive and causes no stress to the patient, a false positive can be detected in the early stages of invasive pneumococcal pneumonia because the test is not as sensitive during mild infections (8). This assay is best performed during the peak of pneumococcal infection, when bacterial counts are high and the infection is quite severe (8). If patients do not deliver adequate sputum samples or have already been on antibiotic therapy, the urinary antigen detection technique can be employed to deliver a definitive result.

Another test, based on DNA sequences that are specific to *S. pneumoniae,* can also be effective in detecting pneumococcal pneumonia (8). These tests employ a very rapid detection technique, and will be quite helpful in future research and clinical developments (8). As of right

now, these assays have a difficult time ascertaining the difference between pneumococci colonization and infection (8). Polymerase chain reaction (PCR) has also been used in the identification of *S. pneumoniae* (20). This molecular detection technique employs species-specific genes to aid in identification (20). For example, the pneumolysin gene, autolysin gene, and pneumococcal surface adhesion gene (*psaA*) have all been used in molecular detection if the pneumococcus (20). The pneumolysin gene has proved to be an inaccurate target because many other members of the *Streptococcus* viridians family have been found to contain this gene, specifically *S. pseudopneumoniae* and *S. mitis*.

Pulmonary function tests may be used in a clinical setting to detect the effectiveness of the respiratory system (17). Malfunctions, such as dyspnea, may occur in patients presenting with pneumococcal pneumonia, thus these tests can be quite useful in determining the severity of their condition (8, 17). Also, pulmonary function tests can be used to ascertain the effectiveness of antibiotic therapy in treating community-acquired pneumonia, among other resources such as a sputum culture to detect the effectiveness of treatment. (17).

Innate Immunity

The innate immune system is the first line of defense against invading pathogens in the human body. The cells and mechanisms comprising the innate immune system defend the body in a non-specific, ubiquitous manner; that is, these cells are not pathogen-specific, nor will they bestow long-lasting immunity like the adaptive arm of the host response. Although the innate immune system is not as specific as the adaptive immune system, the body's first line of defense provides various and immediate mechanisms to deal with the pneumococcus.

The first step in combating pneumococcal pneumonia is recognition by the innate immune system (6, 8). Pattern recognition receptors (PRRs) have the ability to distinguish key components on invading pathogens, referred to as pathogen-associated molecular patterns. When PRRs recognize the invading pneumococcus, they produce inflammatory mediators, such as

TNFα, IL-1β, IL-6, IFNα/β, KC, and MCP-1, which then go on to initiate the acute phase response, control the influx of neutrophils to the infected area, and also control the adaptive immune response (6). Take, for example, the hydrophilic head group of certain phospholipids, phosphorylcholine. In order for *S. pneumoniae* to cross the barrier from lung tissue into blood, phosphorylcholine, which is a component of the pneumococcal cell wall, must bind to a host-derived receptor whose ligand is platelet-activating factor (2, 8). This human ligand also contains phosphorylcholine, thus the bacterium is able to mimic a host cell binding to the receptor (8). C− reactive protein (CRP), an acute phase protein and a PRR for the pneumococcus, has the ability to recognize phosphorylcholine in the bacterial cell wall and activate the classical complement pathway, preventing the pneumococcus from creating a systemic infection (2, 8). CRP directly binds to phosphorylcholine and activates the classical complement pathway through interaction with C1q, a complement component (2). If mice are deficient in this receptor, pneumococcus growth is decreased and there is less of a risk of a systemic infection (8).

Toll-like receptors (TLRs) are also very important members of the pattern recognition receptor family and also the innate immune system (8). These receptors have the ability to activate important transcription factors as well as detect pathogens at the host cell surface, or in lysosomes and endosomes (6, 8). These receptors also activate the adaptive immune response, which makes toll-like receptors vital in the fight against *S. pneumoniae.* There are thirteen known TLRs in mice and ten in humans (6, 21). TLRs can be located on the plasma membrane, such as in TLR1, -2, -4, -5, and -6, or they can be found in endosomes, such as in TLR3, -7, -8, and -9 (6). Transcription factors NF-κB and/or IRF3/7 are activated via toll like receptor's interaction with the four major adaptor molecules, MyD88, TRIF, MAL, and TRAM (6). This is accomplished via a signaling cascade when TLRs associate with the adaptor molecules.

TLR2, often considered to be the most important pattern-recognition receptor for Gram-positive bacteria, has the ability to recognize components of the pneumococcal cell wall,

including lipoproteins and lipoteichoic acid (6, 8). TLR2 is capable of recognizing traits that are specific to Gram positive pathogens, such as large amounts of peptidoglycan, lipoteichoic acid, and bacterial lipopeptides. The the inflammatory response, in the form of an influx of neutrophils to the colonized nasal surface, then follows *S. pneumoniae's* recognition (2, 3, 8). However, TLR2 is not a major contender in the fight against pneumococcal pneumonia (19). Although, TLR2 has been implicated as a major factor in innate immunity in patients with asplenia and functional asplenia (18). In a recent study conducted by Van der Poll, et al, no difference was found between wild-type asplenic murine models and TLR2 knock-out murine models, thus leading to the conclusion that in absence of spleen TLR 2 does not play a greater role in protection against *S. pneumoniae* than in models with a functional spleen (19).

Defects in TLR 9 are implicated in reduced clearance of the pneumococcus from the lungs, leading to augmented bacterial colonization and increased mortality (6, 8). In murine models of infection, TLR 9 $^{-/-}$ knock-out (KO) mice experienced higher mortality rates because TLR 9 is involved in detecting *S. pneumoniae* DNA (6, 8). TLR 9 detects unmethylated CpG DNA structure inside pneumococcal endosomes (6). TLR 9 is also thought to be vital in alveolar macrophages [9], where pneumococci are phagocytized (8).

TLR 4 is another receptor that is active in pneumococcal clearance (6, 8). As demonstrated in TLR 4 $^{-/-}$ KO mice, TLR 4 is crucial for bacterial clearance, upper respiratory tract cell apoptosis, and decreased susceptibility to infection (6). Also, TLR 4 is the receptor responsible for the proinflammatory effects of the pneumococcal exotoxin pneumolysin, and has been implicated in the ability to detect pneumolysin (2, 6, 8). When murine models are infected with high doses of pneumolysin, TLR 4 was active in cytokine and chemokine production (IL-6, IL-1β, KC) along with neutrophil recruitment to the site of colonization (6). Although, TLR 4 is best known for its ability to detect the endotoxin lipopolysaccharide, a component of the outer membrane in Gram- negative bacteria (6). TLR 2, TLR 4 and TLR 9 appear to be active in

controlling pneumococcal infection, although there are still abundant questions to be answered regarding the effectiveness of TLRs in the fight against pneumococcal colonization and infection.

Although defects in TLRs lead to increased susceptibility of pneumococcal pneumonia, animals deficient in the TLR-adaptor protein myeloid- differentiation primary –response protein 88 (MyD88) are tremendously vulnerable to *S. pneumoniae* infection, with MyD88 –deficient mice experiencing a 1000-fold increase in bacterial counts compared to that of wild-type mice (6, 8, 16). This depleted immune response is in part due to decreased innate immune system activation by IL-1 and IL-18, which interact with MyD88 and results in diminished cytokine and chemokine production, increased mortality, sepsis, pneumonia, and bacteremia in models of meningitis (6, 8). Children born with a genetic defect for MyD88 or IL-1 receptor-associated kinase 4 (IRAK4), which is a phosphorylation enzyme that exerts its effect immediately following the MyD88 protein, are also very vulnerable to *S. pneumoniae* infections that are particulary invasive and deadly during early childhood years (6, 16).

The nod-like receptors (NLRs) and inflammasomes are also active in the innate immune response to invasive pneumococcal disease (6, 8, 16). There are twenty-two cystolic NLR proteins, and thirty-three, possibly more, in murine animals (6). Nucleotide-binding oligomerization domain protein (Nod) 1 and Nod2 have been implicated in the detection of the bacterial cell wall component peptidoglycan, which is found in much greater amounts in Gram-positive bacteria such as the pneumococcus (6, 8, 16). Nod1 and Nod2 activate a nuclear transcription factor known as NF- κB, which is a dependent pro-inflammatory gene, after detecting *S. pneumoniae in vitro* (6). Mice that do not express NFκB exhibit reduced clearance of pneumococci in the lungs, and bacterial counts appear higher in NFκB knockout mice (8). Nod2 recognizes and becomes activated by muramyl dipeptide (6, 8). Muramyl dipeptide is a common protein that is a component of the bacterial cell wall peptidoglycan, and can be found in the cytosol of almost all Gram-positive bacteria (6, 16). Once the pneumococcus is internalized by

macrophages it must be digested within lysozymes, and then delivered to the host cell's cytosol, where it is recognized by Nod2 and leads to its activation (6). When *S. pneumoniae* is recognized by Nod2, coupled with the actions of TLR2, an influx of macrophages are recruited to the area of colonization in the upper respiratory tract, through MCP-1 production, thus leading to a faster clearance of the bacterium (6). Also, NOD2 also activates the transcription factor NF- κB, leading to the transcription of proinflammatory genes (6). Type I interferons also appear to be influenced by Nod2 (6). During *S. pneumoniae* colonization, Nod2 seems to contribute to the type I interferon response brought on by colonization (6).

It was originally thought that Nod1 was not important in pneumococcal pneumonia because it recognizes peptidoglycan fragments, specifically meso-diaminopimelic acid (mesoDAP)-containing muropeptides, that are common to Gram-negative bacteria, but Jeff Weiser's lab provided some insight on the topic (6, 16). Interestingly, Gram negative bacteria that are a component of the natural gut flora produce mesoDAP-muropeptides that enter the systemic circulation and activate an influx of neutrophils, which can then be used to defend against invasive pneumococcal disease (16). Therefore, the extraneous use of broad-spectrum antibiotics for example, which kill the normal gut flora, may make an organism particulary vulnerable to invasive pneumococcal disease, once again stressing the seriousness of unnecessary antibiotic use (16).

Inflammasomes are protein complexes that are formed after the recognition of a wide array of stimulants from the various NLRs, including NLRP1, NLRP3, and NLRC4 (15). After inflammasomes are formed, activation of the enzyme caspase-1 follows that secretes cytokines IL-1β, IL-18, and IL-33, which are critical to the innate immune response of the host (8). Pneumolysin (PLY) is critical for the activation of caspase-1 and thus the formation of the subsequent cytokines (6). These inflammasomes are also crucial from a post-translational modifications standpoint; they cleave IL-18 and IL-1β, thus producing functional cytokines from

their non-functional zymogenic counterparts, also known as the pro-form of the molecule (6). NLRP3 knockout mice have a greater morbidity rate, most likely due to the influence NLRP3 exerts on bacterial clearance in the lungs (6). This inflammasome-producing protein appears to control the rate of bacterial clearance in the lung (6). NLRP3 is also responsible for maintaining the integrity of the endothelial and epithelial barriers in the lung tissue (6). Finally, the NLRP3 inflammasome has been shown to be involved in IL-1β production in macrophages and dendritic cells (DCs), a process that is stimulated by the exotoxin pneumolysin (6). AIM2 is another inflammasome-producing protein that influences IL-1β production in infected host macrophages (6). When IL-1β, IL-1, or IL-18 production is impaired in murine models, the animals experience a much greater susceptibility to *S. pneumoniae* invasion (6).

Another important factor in host recognition of the pneumococcus, often considered the link between the innate and adaptive immune response, is dendritic cells (DCs) (14, 20). Dendritic cells are antigen-presenting cells (APCs) that will engulf, digest, and process the pneumococcus. The maturation of DCs is characterized by the production of cytokines, which promote the immune system response. DCs, through the action of cytokines, have the ability to alert and activate the innate immune response (21). Also, DCs are capable of initiating the adaptive immune response by trafficking to lymphoid organs, which house naïve T cells, and promoting clonal expansion of naïve T cells (14, 22, 23). Until recently, human dendritic cells were associated with the bacterial exotoxin pneumolysin, which punches holes into host cells and induces an inflammatory response (15). However, research has shown that human DC infection with the pneumococcus, which expresses pneumolysin, promotes formation of proinflammatory cytokines, DC apoptosis, activation of inflammasomes, and inhibition of host DC.

Acquired Immunity

Acquired immunity, also referred to as pathogen-specific immunity, is the highly adaptable second line of defense for the body. When the pneumococcus is not contained within its carrier

niche in the nasopharynx, it can infiltrate the lower bronchi and cause invasive pneumococcal disease (2, 3, 8). In order for the body to effectively clear this invasive pathogen, the innate and acquired immune responses must be orchestrated together. Upon presentation of pneumococcal antigens using dendritic cells and macrophages, B and T cell pathogen-specific populations develop and migrate from the inductive site, through the systemic circulation, and settle on the mucosal surface of the nasopharynx, also known as the effector site (24). By employing the pathogen-specific arm of the immune system, the body can activate serotype-specific antibodies coupled with the complement system for opsonization and, increasingly gaining more interest, CD4+ T cells in the fight against *S. pneumoniae* (2, 16, 24).

During the initial host colonization, it has been shown that CD4+ T cells have the ability to recognize pneumococcal surface antigens (7). Using a murine model of pneumococcal disease, researchers were able to prove that TLR2-dependent, antibody-independent CD4+ T cells lead to increased T-cell infiltration in the infected lung, and also produce IL-17A, which has been shown to increase macrophage and neutrophil influx to the nasopharynx through granulopoeisis and chemokine induction, and assist in pneumococcal clearance during colonization and primary infection (2, 7, 8, 16, 25). During pneumococcal colonization, CD4+ T-cell-deficient mice were not able to clear the pneumococcus, which could be due, in part, to the lack of a T helper 1 (Th1) response (2). Induction of the Th1 response has previously been shown to protect humans from invasive pneumococcal disease (2). In order for the host to accumulate large amounts of T cells in the lungs at such an early stage of disease, pneumolysin must be expressed by the pneumococcus (8). It has been shown that pneumolysin-deficient pneumococci fail to stimulate the T-cell migratory process and will not induce CD4+ T cell-dependent clearance, while pneumococci that express pneumolysin are successful in stimulating the migratory process and clearance (2). When CD4+ T cells are less-than-adequate in numbers, patients experience a 50-fold greater risk of developing invasive pneumococcal infections as well as other respiratory

infections (2, 7). Loss of memory B cells, decreased pulmonary immunity, and decreased activity of anticapsular antibodies are a few mechanisms that are affected with low CD4+ T cell numbers (7). Additionally, CD4+ $^{-/-}$ mice, which lack MHC Class II molecules, experience greater bacterial loads than mice with normal CD4 $^{+}$ T cell counts (2, 25). In a model of pneumococcal carriage, it has been demonstrated that antibody-deficient mice were protected against pneumococcal colonization, but CD4+ T cell-deficient mice were not protected (2, 25). These results were observed two months after immunization, dispelling any notions that these results are a product of innate immunity and showcasing the involvement of CD4+ T cells in long-lasting immunity (25). It is not yet understood how CD4+ T cells precisely protect against pneumococcal colonization, but a few theories have been suggested (25). For example, CD4+ T cells have been implicated in generating the Th1 response through TLR4 ligands, which have been shown to favor the Th1 response (25). Thus, instead of the notion that each ST, based on the antigens presented in the capsule, presents a different pathogen for the host immune system to eradicate, it may now be appropriate to consider the host serotype-independent and elucidate a common mechanism across all pneumococcal serotypes (2).

The humoral immune response includes the interactions of B cells with T cells, and the differentiation of naïve B cells into antibody−producing plasma cells. The antibody response has been implicated as one of the crucial immune functions mediating pneumococcal clearance. Since *S. pneumoniae* is an extracellular pathogen, class−switched, anti−capsular antibodies specific to each serotype must be produced to mark the pathogen for destruction. Thus, strategies to increase the humoral immune response to *S. pneumoniae* pathogens may confer a large degree of protection to invasive pneumococcal disease.

The first step to invasive pneumococcal disease is carriage within the nasopharynx. This colonization step typically happens within the first two years of life, and can lead to the development of serotype−specific antibodies (7). However, it is unclear as to whether the

development of anti−capsular antibodies results in resistance to pneumococcal colonization later in life, or contributes to the decline in colonization as children age (26).

Vaccination strategies have been utilized around the world to minimize the incidence of *S. pneumoniae* colonization and disease progression. Currently, the 7−valent, 13−valent, and 23−valent polysaccharide conjugate vaccines are in use by health professionals (27). These vaccines target the polysaccharide capsule of the most prevalent serotypes, as determined by assessing clinical isolates from human patients (11). However, there has been a large movement to develop a vaccine that targets all clinically relevant STs, since the conjugate vaccines are only protective against certain STs. A serious contender for a pan−serotype pneumococcal vaccine is pneumolysin, a virulence protein expressed on all clinically relevant *S. pneumoniae* serotypes (28). Novel, protein−based vaccines that target all pathogenic pneumococcal STs are currently in development.

Introduction to Vitamin A

The retinoids (vitamin A) are required in numerous in biological processes including epithelial barrier maintenance and integrity, immune function, vision, reproduction, and normal growth and development (29, 30). In addition to the many physiological functions vitamin A (VA) and its metabolites participate in, its active vitamer retinoic acid (RA) is essential in the regulation of over 500 proposed genes (30). VA can be found in the diet as two forms – preformed vitamin A, which consists of retinol and retinyl esters, and pro vitamin A, which contains the carotenoids β−carotene, α−carotene, and β−cryptoxanthin (29). Retinoids and carotenoids are widely distributed in foods, but liver, margarines, and fortified foods have the highest level of preformed VA, which is found predominately as retinyl esters (REs). Provitamin A is found in abundance in colorful vegetables, such as spinach, squash, and carrots. Normal digestion in the duodenum of the small intestine is required to release VA from the complex matrix of food, releasing primarily REs as the final degradation product. REs must be hydrolyzed by retinyl ester hydrolase (REH), either in the lumen of the intestine or at the apical membrane of the enterocyte (30). Free retinol (ROH) and a fatty acid (FA), usually palmitate, are released as products of REH digestion. Since VA is hydrophobic, and thus lipid soluble, VA digestion is optimized when consumed with dietary fats, as this promotes emulsification with bile salts and dietary FAs, incorporation into micelles, and uptake of VA into the enterocyte. ROH will be incorporated into micelles along with other products of digestion, such as cholesterol, dietary FAs, and bile salts, and absorbed into the enterocyte via passive diffusion. It is postulated that β−carotene, a form of provitamin A, will be taken up into the enterocyte via the scavenger

receptor SR-B1, and once within the enterocyte it can be cleaved centrally by cytosolic 15, 15' dioxygenase to form two molecules of retinal. Retinal can then complex with cellular retinol binding protein II (CRBP II) located in the cytosol (29, 30). Retinal can be reduced by retinal reductase to ROH, which will also complex with CBP II.

Although VA is a biologically essential micronutrient, it is highly toxic to the body and thus must always be associated with a binding protein (BP) or chaperone protein when being shuttled through the vasculature or tissues in order to prevent the retinoids from causing damage to cell membranes. Furthermore, the BP provides solubility to the insoluble retinoids, allowing them to be transported to the tissues (29). Therefore, once ROH enters the enterocyte it will immediately complex with cellular retinol binding protein II (CRBP II). Once bound to CRBP II, the ROH-CRBP II complex is now an appropriate substrate for lecithin: retinol acyltransferase (LRAT) (29, 30). LRAT catalyzes the formation of REs by esterifying a long-chain fatty acid (LCFA), typically palmitic, stearic, or oleic acids, to CRBP II- bound ROH (29). At physiologic concentrations of VA, LRAT is capable of esterifying all of the bound ROH so that its product can be incorporated into nascent chylomicrons (29). However, large bolus doses of VA, either as pro- or preformed VA, are capable of saturating CRBP II and thus limiting the activity of LRAT. Therefore, the body employs an overflow mechanism, also known as acyl COA: retinol acyltransferase (ARAT). ARAT does not require CRBP II-bound ROH as a substrate; rather, free ROH can be esterified with a LCFA to form REs and be incorporated into chylomicrons for subsequent transit through the lymphatic system (29). Nascent chylomicrons are secreted into the lymphatic system and rapidly hydrolyzed into remnant chylomicrons, which are cleared by the liver (30). Also, a small portion of ROH may be secreted from the enterocyte and bound to retinol binding protein (RBP) in the plasma, although this is not a major means of excretion from the enterocyte (29). The chylomicron remnants enter the hepatocyte through the space of Disse, and are sequestered by heparin sulfate proteoglycans and subsequently taken up by hepatic lipase

(HL), or the remnant will bind to the LDL receptor (LDLR) via its apo E moiety, depending on the physiologic state of the individual (29, 30). It is proposed that the REs are subsequently hydrolyzed by carboxylesterase ES10 located on either the endoplasmic reticulum (ER) or endosomes (29). Although the exact mechanism is unclear, ROH is trafficked to the hepatic stellate cells, which are specific for RE storage, presumably bound to CRBP I (29, 30). It has been shown that mutant mice with a CRBP I deficiency have a 50% decrease in levels of retinyl palmitate, which is the primary fatty acyl group esterified with ROH (29, 30). Hepatic stellate cells highly express the ROH-esterifying enzyme LRAT, and the newly formed REs are stored in lipid droplets in the stellate cells. mRNA expression of LRAT in liver stellate cells is directly proportional to VA status (29). Thus, in time of VA adequacy (VAA) humans will store a very large portion of their VA (~ 90%), while during times of VA deficiency (VAD) LRAT activity is greatly reduced in the liver, due to the decrease in transcription of LRAT mRNA (29).

When VA must be mobilized from the liver for use in other tissues, retinyl ester hydrolases (REHs) work on the REs and release free retinol into the circulation (31). In tissue, ROH is converted to retinal, and terminally oxidized to RA. RA can then perform the physiological functions of VA. RA has many functions in tissue development, embryogenesis, reproduction, and vision, but this review is primarily concerned with RA's role in immune system development and function.

RA acts by binding to nuclear receptors found within the promoter of genes, and represses or induces the transcription of mRNA (32). The retinoic acid receptor (RAR) heterodimerizes with the retinoid X receptor (RXR) in regions of the DNA referred to as retinoic acid response elements (RAREs) (33). The RAR family contains three members: RAR alpha, RAR beta, and RAR gamma (33). RA has numerous functions in the immune system such as, leukocyte homing, plasma cell differentiation, inducible T regulatory cell induction (iTregs) and effector CD4+ T cell subset differention.

Leukocyte homing is a process by which immune cells traffic to injured or infected areas of the body through the use of chemotactic molecules (i.e., cytokines) and the coordinated expression of adhesion molecules. CD103+ (mucosal) DCs are capable of synthesizing RA from ROH, and the presence of RA increases the expression of the gut homing markers α4β7 and chemokine receptor 9 (CCR) on T cells (34). That is, when the T cell receptor is engaged by RA−producing DCs, activated T cells display increased expression of gut homing markers, which increase the migratory ability of T cells to the lamina propria. Furthermore, Song et. al. (34) discovered that vitamin A deficient (VAD) mice had reduced α4/β7+/CD4+ activated T cells in secondary lymphoid organs (spleen, lymph nodes, etc.), and, interestingly, VAD mice contained normal T cell populations in the liver and lung, but intestinal lamina propria T cells were completely depleted. Thus, RA is essential for the induction of gut homing markers to the intestine.

Moreover, RA has crucial roles in IgA−secreting plasma cell differentiation and function (33). Plasma cells are an "antibody−producing factory", and are essential in the clearance of extracellular pathogens and foreign bodies. IgA is an antibody commonly found at mucosal surfaces and in bodily secretions, and is most often found in its secretory, dimeric form (35). In the blood, IgA can also interact with CD89 present on immune effector cells to induce a respiratory burst in granulocytes, and de−granulate mast cells, basophils, and eosinophils, triggering an inflammatory reaction (35). It was discovered that RA also plays an essential role in IgA−secreting plasma cell function. RA and IL−5/IL−6, produced from mucosal DCs, synergized to induce the expression of gut homing markers and secretory IgA from B cells (36). VAD mice did not contain IgA−secreting plasma cells in the small intestine, further implicating RA in gut homeostasis and tolerance (36).

RA is also critical for CD4+ T (Thelper) cell differentiation and function. Thelper cells promote the adaptive immune response by "helping" other facets of the immune system function.

For example, CD4+ T cells are critical for antibody class−switch, CD8+ T cell (cytotoxic T lymphocyte) activation and growth, and macrophage function. Historically, CD4+ T cells were divided into two categories: Th1 or Th2. A Th1−skewed T cell response is essential for intracellular pathogen clearance, and the signature Th1 cytokine is interferon gamma (IFN γ). Conversely, a Th2−skewed response is necessary for host defense against extracellular invaders, and the polarizing cytokine is IL−4. VA is known to promote a Th2−skewed response and the signature cytokines IL−4 and IL−5 by acting through RAR−RXR to increase expression of the transcription factor GATA3, which acts to increase the transcription of genes that promote Th2 CD4+ T cell differentiation (37).

Additionally, RA is known to affect another CD4+ T cell subset, referred to as Th17 cells. Th17 cells comprise a recently discovered Thelper cell subset that is present at mucosal surfaces. They secrete IL−17A and IL−17F, which act to increase neutrophil influx to a site of injury or infection. Th17 cells have recently been implicated in the development of autoimmune and allergic diseases, and are known to cause tissue damage and inflammation at a site of injury. In the presence of TGF−β and IL−6, naïve T cells differentiate into Th17 cells and begin secreting IL−17, IL−23, IL−22, IL−6, and TNF−α (37). In the presence of RA and TGF−β, naïve T cells will oppose Th17 cell commitment and differentiate into Tregulatory cells, which promote an immunosuppressive environment and discourage the development of autoimmune cells (38). RA acts to decrease the expression of the IL−6 receptor and increases TGF−β signaling, effectively shifting the balance towards a Treg cell−skewed phenotype (39).

Finally, RA is known to induce the differentiation of naïve T cells into T regulatory cells. Forkhead box protein 3 (Foxp3) is the “master transcriptional regulator” that controls the differentiation of T regulatory cells. Regulatory T cells are critical for tolerance to self−antigens the modulation of immune system function, especially the inflammatory response. There are two

subsets of Tregulatory cells: natural and inducible Tregs. Natural Treg develop in the thymus, and are a committed regulatory T cell that expresses Foxp3 as they migrate from the thymus into the periphery (40). Conversely, inducible Tregs (iTregs) are uncommitted as they emerge from the thymus, and differentiate into Tregs in the periphery (40). In the presence of TGF−β, RA, and low levels of IL−6 iTregs will develop and act to suppress the immune response, contributing to immune homeostasis (37). Additionally, Foxp3 can bind to and directly inhibit the action of the Th17 cell nuclear receptors, RORα and RORγτ, effectively halting the transcription of Th17 cell−associated genes (37).

Chapter 2

Rationale, Hypotheses, and Aims

Rationale

Pneumonia is an inflammatory condition of the lower respiratory tract that can be contracted from numerous pathogens such as bacteria, viruses, parasites, or fungi. Idiopathic (noninfectious) pneumonia can also arise, but these cases are much less common than pathogen−induced pneumonia. *Streptococcus pneumoniae*−induced pneumonia is a major public health concern in both the United States and developing countries, contributing to 1.6 million deaths annually worldwide (41). Pneumococcal pneumonia can affect all populations, but infection is most frequently observed in immunocompromised, elderly, and very young (< 5 years of age) patients (41). Bacterial pneumonia infection claims the lives of approximately 800,000 children per year, and the majority of those deaths are concentrated in the poorest countries (2).

The VA status of neonates is naturally low, and status is further compromised in premature infants and maternal vitamin A deficiency (VAD). Therefore, the World Health Organization (WHO) recommends VA supplementation in bolus dose capsules to children 6 months to 5 years of age (42). However, the WHO does not recommend VA supplementation in 0−6 month old neonates due to insufficient data regarding bolus dose supplementation toxicity. VA, in the form of RA, is critical for both immune system maturation and normal lung development during the neonatal period. Thus, studies on neonatal VA supplementation are required to elucidate the efficacy of supplementation and its effects on immune system maturation, lung development, and overall health of the newborn.

We propose that VA supplementation in the neonatal period will reduce the burden of *S. pneumoniae* ST3 and ST14 in the lung of infected mice by regulating the innate and adaptive immune response. VA is transformed through multiple conversions in tissue, until it undergoes its terminal oxidative reaction to RA. RA acts as a transcriptional regulator by binding to retinoic acid responsive elements (RAREs) located in the promoter of genes and influences mRNA transcription. We hypothesize that the poor VA status observed in neonates causes a decreased antibody response and reduced Treg cell populations, leading to increased bacterial load and inflammation, respectively. Therefore, VA status may be a primary factor contributing to the increased mortality and morbidity observed in neonatal patients infected with pneumococcal pneumonia.

Question: Does early life VA supplementation reduce the burden of *S. pneumoniae* S 3 or ST14 infection in the lung and blood of neonatal mice?

Hypothesis: VA supplementation to vitamin A marginal (VAM) neonates will induce the differentiation of antibody−producing plasma cells during primary *S. pneumoniae* infection and thus promote faster pathogen clearance.

Specific Aim 1: Measure, by quantitative plate counts, lung and blood colony forming units (CFUs) during *Streptococcus pneumoniae* S 3 or ST14 infection in VAM and VAM + VA supplement treatment groups.

Question 2: Does VA supplementation during the neonatal period change the immune cell populations present in the lung during an acute *S. pneumoniae* ST3 or ST 4 infection?

Hypothesis: VA supplementation to VAM neonates will increase the B cell and myeloid populations in the lung during acute pneumococcal infection with ST3 or ST14.

Specific Aim 2: Measure, via flow cytometry, the changes in the aforementioned immune cell populations in the lung during pneumococcal pneumonia infection with ST3 or ST14 in VAM and VAM + VA supplemented neonatal mice.

Question 3: Do the immune cell populations present in the lung differ between infection with *S. pneumoniae* ST3 and ST14?

Hypothesis 3: Infection with *S. pneumoniae* ST14 causes a massive granulocyte infiltration to the lung, while ST3 infection causes little immune cell migration and lung infiltration.

Specific Aim 3: Measure, via flow cytometry, the changes in neutrophil, macrophage (mϕ), NK, and NKT cell populations in the lung during pneumococcal pneumonia infection with ST3 or ST14. Additionally, a myeloperoxidase assay will be used to assess neutrophil activity.

Chapter 3

Materials and Methods

Animals. Adult (8−12 weeks old) male and female Balb/c mice were purchased from Charles River Laboratories, and housed in a specific pathogen-free facility under a 12:12−h dark-light cycle. Animals were kept in polystyrene vented cages at 22° C with free access to food (see below) and water. All procedures for animal care and experimental use were in accordance with the Pennsylvania State University's Institutional Animal Care and Use Committee (IACUC#41454).

Breeding. Harem mating (2 adult females, 1 adult male) was used to generate litters. Adult (8-week-old, n=2) Balb/c dams were bred with adult (8−12 weeks old, n=1) Balb/c males under the above conditions. After 10 days the animals were separated and placed in individual cages with ad libitum access to food and water (see next section for detailed diet information). After gestation and birth, litters were not disturbed for four days. On postnatal day 4 (pnd 4), pups were examined for sex and appropriately cross−fostered to generate randomized treatment groups and eliminate a litter effect.

Diets. Adult male mice were fed a standard chow diet (Rodent Diet 5001; Purina Laboratory) for all experiments. After breeding, dams were placed on a vitamin A−marginal purified diet (0.35 μg retinol/g, AIN−93G diet; Research diets, New Brunswick, New Jersey) to reduce the transfer of VA in milk to pups in order to generate VAM pups. Dams and pups remained on the VAM diet for the duration of the VA supplementation experiments. To mimic the bolus dose VA

supplement used in children > 6 months old, randomly selected pups were directly fed either vehicle (canola oil; control) or VA supplement (1550 μg retinyl palmitate, Sigma, dissolved in 10 μl canola oil) on pnd 12. Treatment was administered in two doses, pnd 12 and 13, prior to infection using a positive displacement pipette. For the *S. pneumoniae* ST3 and ST14 comparison studies, all animals were fed the standard chow diet.

Neonatal pneumonia model. *S. pneumoniae* ST3 (ATCC 6303) was reconstituted in 1 ml Todd−Hewitt broth (THB) and grown for 24 h at 37° C and 5% CO_2 or until log−phase growth was reached. A loopful of log−phase bacteria was streak plated on Trypticase soy agar plates with 5% sheep's blood (BD Diagnostic Systems, Sparks, MD) and grown overnight (O/N) at 37° C and 5% CO_2. After overnight growth, an isolated colony was chosen and grown in THB for 6 h or until mid−log phase was reached. Mid−log phase cultures were frozen in 0.5 ml and 1 ml aliquots at −80° C in 25% glycerol as working stock. *S. pneumoniae* ST14 (ATCC 6314) was reconstituted in 1 ml Brain Heart Infusion (BHI) broth and growth for 24 h at 37° C and 5% CO_2 or until log−phase growth was reached. A loopful of log−phase bacteria was streak plated on Trypticase soy agar plates with 5% sheep's blood (BD Diagnostic Systems, Sparks, MD) and grown overnight (O/N) at 37° C and 5% CO_2. After overnight growth, an isolated colony was chosen and grown in BHI broth for 6 h or until mid−log phase was reached. Mid−log phase cultures were frozen in 0.5 ml and 1 ml aliquots at −80° C in 25% glycerol as working stock. Pups were dosed, via direct mouth feeding with a positive displacement pipette, with VA supplement or vehicle one time per day 2 days before the inoculation (pnd 12 and 13). Prior to each infection study, an aliquot of frozen ST3 or ST14 working stock was thawed at room temperature and centrifuged at 1500 x *g* for 15 min at 4° C and washed twice with 1x DPBS. Mice were anesthetized with isoflurane and intranasally inoculated with $1x10^3 - 1x10^7$ CFUs of ST3 or ST14 in 20 μl 1x DPBS. The pup's jaw was gently closed shut, and the inoculating dose

was placed directly on the nares of the neonates, which forced them to inhale the pathogen directly into their lungs. The infectious dose administered in each experiment is noted in the figure legends. Non−infected control mice were sacrificed before each inoculation. Infected mice were monitored twice daily for signs of distress such as labored breathing, disheveled appearance, dehydration, and weight loss. If weight loss was greater than 20% of original body weight, animals were euthanized by CO_2 asphyxiation and vena cava blood was collected. Pneumonia pathogenesis and disease severity was monitored at 4 h, 12 h, 24, 48, and 72 h post−infection (p.i.). At selected time points, animals were subjected to CO_2 asphyxiation and vena cava blood, lung, and liver was collected. Whole blood was used to determine the extent of bacteremia. The liver and small portion of the right lobe of the lung was snap frozen in liquid nitrogen and stored at −80° C for Ultra−performance liquid chromatography (UPLC) and mRNA analysis, respectively. The remaining portions of the lung were sectioned as described below and used for the following assays: the complete left lobe of the lung was stored on ice and used for flow cytometry and the remaining portion of the right lobe was stored on ice and used for CFU determination and a MPO assay.

Pneumococci recovery from the lungs and blood. A portion of the right lobe of the lung was homogenized in 1 ml of PBS (part 1), and serially diluted in a 1:10 dilution scheme. 20 μl of homogenates were plated on Trypticase soy agar plates (BD Biosciences) containing 5% sheep's blood and grown O/N at 37° C and 5% CO_2. 10 μl of whole blood was plated on Trypticase soy agar plates (BD Biosciences) containing 5% sheep's blood and grown O/N at 37° C and 5% CO_2 to determine the extent of bacteremia. Bacterial colonies were counted the following morning. In later infection studies (part 2) a portion of the right lobe of the lung was homogenized in PBS according to lung weight (i.e., 1 mg tissue = 1 μl PBS), and utilized as described above. The

remaining lung homogenate was frozen at −80° C and used in MPO assays to determine neutrophil activity.

Flow cytometry preparation and analysis. The left lobe of the lung was minced on a wire mesh grid in 10 ml of PBS. The resulting cell suspension was filtered through 80 μm nylon mesh, and centrifuged at 1500 rpm for 10 min at 4° C. Cell suspensions were aspirated and subjected to red blood lysis. The cells were then centrifuged at 1500 rpm for 10 min at 4° C, aspirated, and resuspended in 1 ml of flow buffer (PBS + 1% BSA + 0.05% Sodium Azide). Two x 10^5 aliquots of cells were resuspended in flow buffer and stained with 0.1 μg of antibody. The following combinations were used in the various experiments (table 1):

Immune cell populations	Antibody	Conjugated fluorochrome
Lymphocytes/granulocytes (part 1)	anti–Gr–1	FITC
	anti–B220 OR CD19	PE
	anti–CD45	PECy7
	anti–CD3	Alexa647
Myeloid populations (part 1 & 2)	anti–CD11b	PE
	anti–CD11c	FITC
	anti–CD45	PECy7
	anti–F4/80	APC
NK/NK T cells (part 2)	anti–CD27	PECy7
	anti–CD49b	APC
	anti–CD3	FITC
	anti–CD11b	PE

Table 1: Flow cytometry antibodies used

Cells were stained for 60 minutes in the dark at room temperature, washed with flow buffer, washed at 1500 rpm for 5 min at 4° C, and fixed in 75 μl of fixative (4% paraformaldehyde) for a

minimum of 30 min. Samples were run on an Accuri C6 flow cytometer (Accuri, BD Biosciences, San Jose, CA), and channels were optimized for each fluorochrome used. Unstained samples (negative control) were prepared from pools including the control and treatment groups and used to set up the live-cell gate, and determine the parameters of background staining versus positive staining for each antibody used. Cells were stained with single, isotype−matched antibodies (positive control) to set the appropriate compensation for samples stained with multiple antibodies.

Myeloperoxidase (MPO) assay. Lung homogenates were thawed at room temperature, and a 100 µl aliquot was removed and mixed with equal volume 1% hexadecyltrimethylammonium bromide buffer (1% hexadecyltrimethylammonium bromide in 50 mM potassium phosphate buffer, pH 6.0). Samples were vortexed vigorously for 1 min, frozen at −80° C, thawed in a 37° C water bath, and vortexed again for 1 min to extract the enzyme. Samples were then centrifuged at 5000 x g (6080 rpm in Beckman centrifuge) for 30 min at 4° C, and the supernatant was collected. In a 96 well plate, samples were 3−fold serially diluted in potassium phosphate buffer. Afterwards, *O*−dianisidine HCL solution (*o*−dianisidine HCL and 50 mM potassium phosphate buffer, 0.334 mg/ml) was added to the samples to achieve a final concentration of 0.167 mg/ml. Standard (commercial MPO, BD Biosciences) was 2−fold serially diluted to yield a standard curve. One percent hydrogen peroxide was added to the standard and samples to initiate the enzymatic reaction. After 30 s, samples were read on a plate reader at 450 nm. The second dilution was used for sample analysis.

Ultra−performance liquid chromatography (UPLC). To determine VA status of the neonates, liver retinyl esters were quantified in tissue homogenates by UPLC. Briefly, lung tissue was weighed, homogenized and subsequently extracted in a chloroform:methanol (2:1, v/v) solution

overnight. Tissue extracts were filtered, rinsed, and washed the following morning. Trimethylmethoxyphenyl−retinol was used as the internal standard, and added to portions of total lipid extracts. Samples were then dried and reconstituted in chloroform:methanol (1:1) solution for UPLC analysis. Approximately 7 μL sample volume was injected onto a C−18 reverse−phase UPLC column, and eluted with 90:10 methanol−water and eventually 100% methanol (gradient mobile phase). The eluted sample was analyzed at 325 nm.

Statistics. Two−way analysis of variance (two−way ANOVA) with Bonferroni's multiple comparisons post−hoc test was used to analyze lung and blood CFUs, and flow cytometry and myeloperoxidase data. Body weight data was analyzed by a two−tailed t−test with Tukey's post−hoc analysis. UPLC data was analyzed by a one−way ANOVA with Tukey's multiple comparisons post−hoc test. All statistical analyses were performed used GraphPad Prism software (version 6.0, La Jolla, CA), and a *P* value of less than 0.05 was considered significant.

Additional note. The experiments performed were a combined effort of a few members of the Ross lab, including myself. I was primarily responsible for animal care, lung and blood CFU determination, and the MPO assay. Flow cytometry prep and analysis was divided amongst myself, Qiuyan Chen, MD., Ph.D., and Katherine Restori, Ph.D. Nan Qi Li, Ph.D. performed the UPLC analysis. Conceptualization and experimental design was a combined effort of myself, A. Catharine Ross, Ph.D., and Katherine Restori, Ph.D.

Chapter 4

Results

Part 1: VA supplementation before an acute *Streptococcus pneumoniae* infection in neonatal mice

Experimental design

Neonatal mice were supplemented with retinyl palmitate or vehicle one time per day for 2 days (pnd 12 and 13) immediately before inoculation with *S. pneumoniae* ST3 or ST14 (pnd 14). The experimental design is illustrated in figure 1.

Figure 1: Experimental design for VA supplementation studies

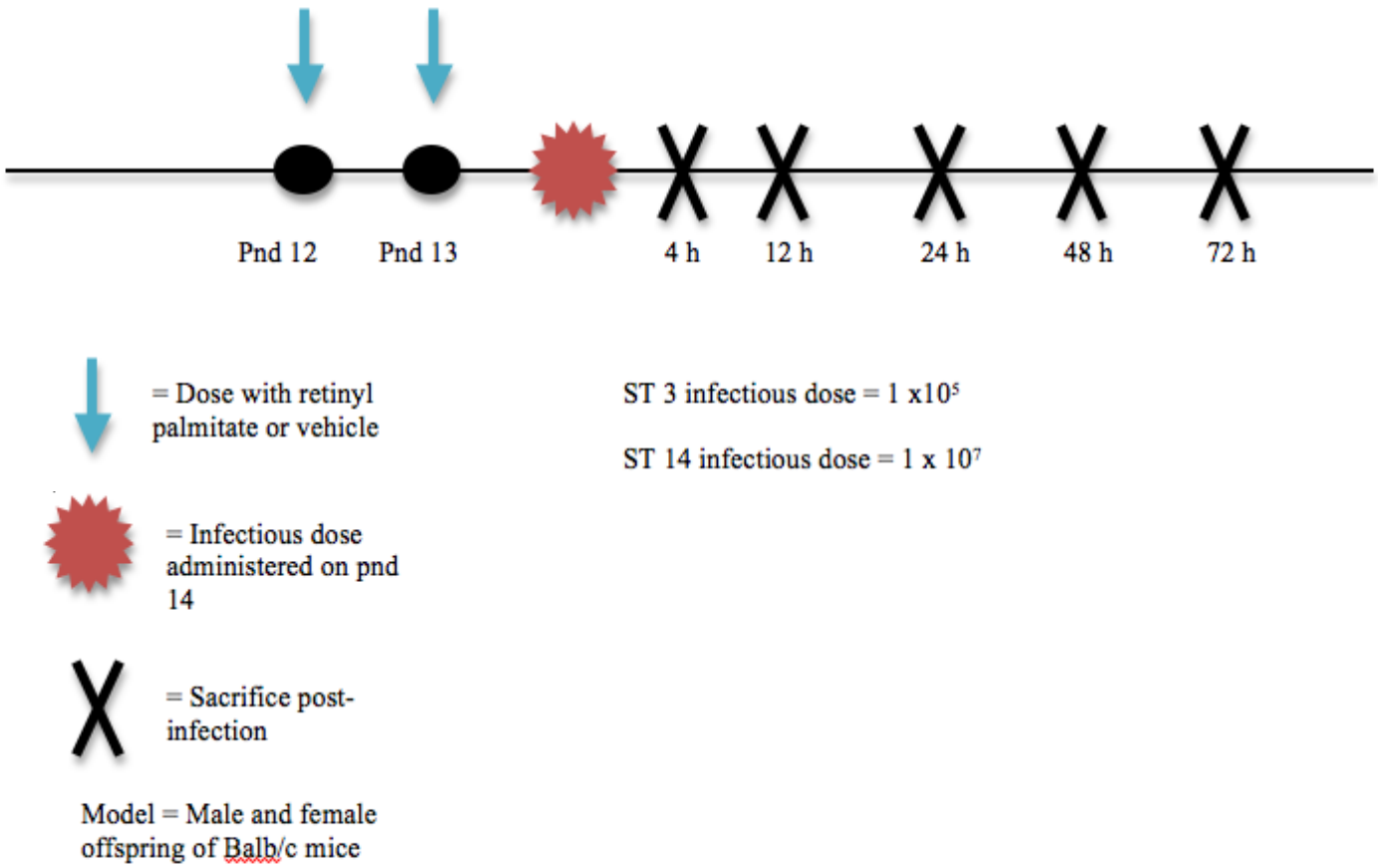

Body weights

After inoculation, mice were sacrificed at various time points and examined for changes in body weight (Figure 2).

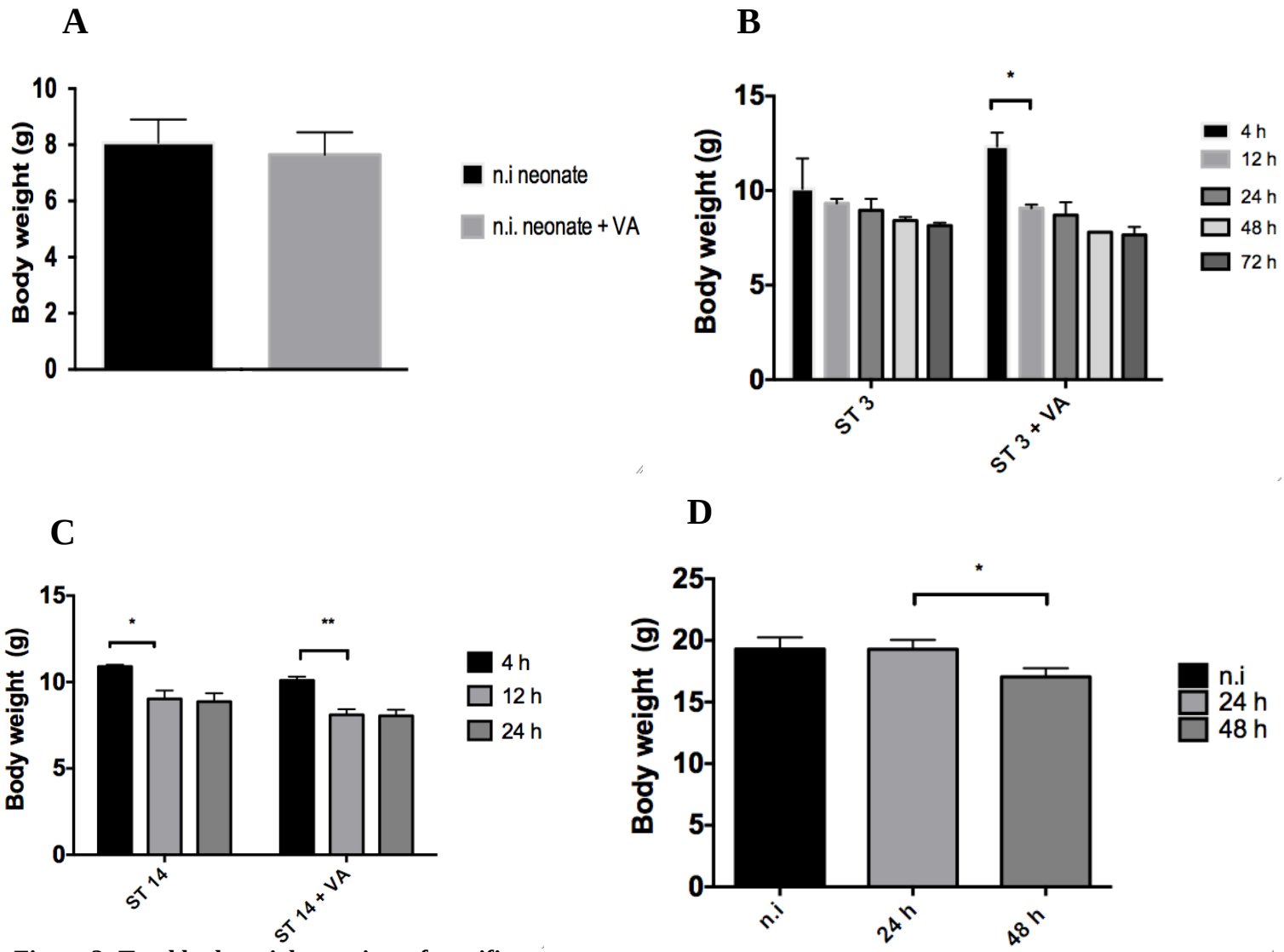

Figure 2: Total body weights at time of sacrifice

Animals were dosed with either retinyl palmitate or vehicle, and subsequently inoculated with 1 x 10^5 CFUs of *S. pneumoniae* ST3 or 1 x 10^7 CFUs of *S. pneumoniae* ST14. Animals were sacrificed at various time points. Bars represent ± SD of 3 independent *in vivo* experiments (n = 12−15 animals per treatment group). Stars indicate statistically significant differences as analyzed by two−tailed t−test and Tukey's post hoc test. $P < 0.05$ was considered statistically significant. A) Non−infected (n.i) controls were sacrificed before inoculation. B) Neonates (pnd 14) infected with 1 x 10^5 CFUs ST3. C) Neonates (pnd 14) infected with 1 x 10^7 CFUs ST14. D) Adult (8 wk) females infected with ST3 at 1 x 10^5.

Retinyl palmitate supplementation had no effect on pup body weight (Figure 2A). However, pups infected with *S. pneumoniae* ST3 and treated with VA experienced a significant decrease in body weight from 4 to 12 hours p.i, while the body weights of pups infected with ST3 and dosed with vehicle did not significantly increase or decrease (Figure 2B). Mice infected with ST14 exhibited a decrease in body weight from 12 to 24 hours p.i. irrespective of treatment (Figure 2C), while adult female mice inoculated with ST3 showed a drop in body weight from 24 to 48 hours p.i.

Lung and blood bacterial load during acute phase pneumococcal pneumonia

In order to assess pneumococcal colonization, lung homogenates were serially diluted, plated on blood agar plates, and grown overnight. Pneumococcal colonies were then measured to determine the extent of bacterial burden at the primary infection site (Figure 3). Treatment with retinyl palmitate (VA) had no effect on bacterial burden 4, 12, or 24 h p.i (Figure 3A, 3B, and 3C, respectively). However, animals infected with ST14 had a much greater bacterial recovery at 4 h p.i than 24 h p.i ($P < 0.05$) (Figure 3D). Similarly, lung CFU counts were significantly decreased at 12 h p.i compared to 4 h p.i ($p < 0.01$) (Figure 3D). Bacteremia, as determined by whole blood CFU analysis, was generally not present at any time point and presence was independent of treatment (data not shown).

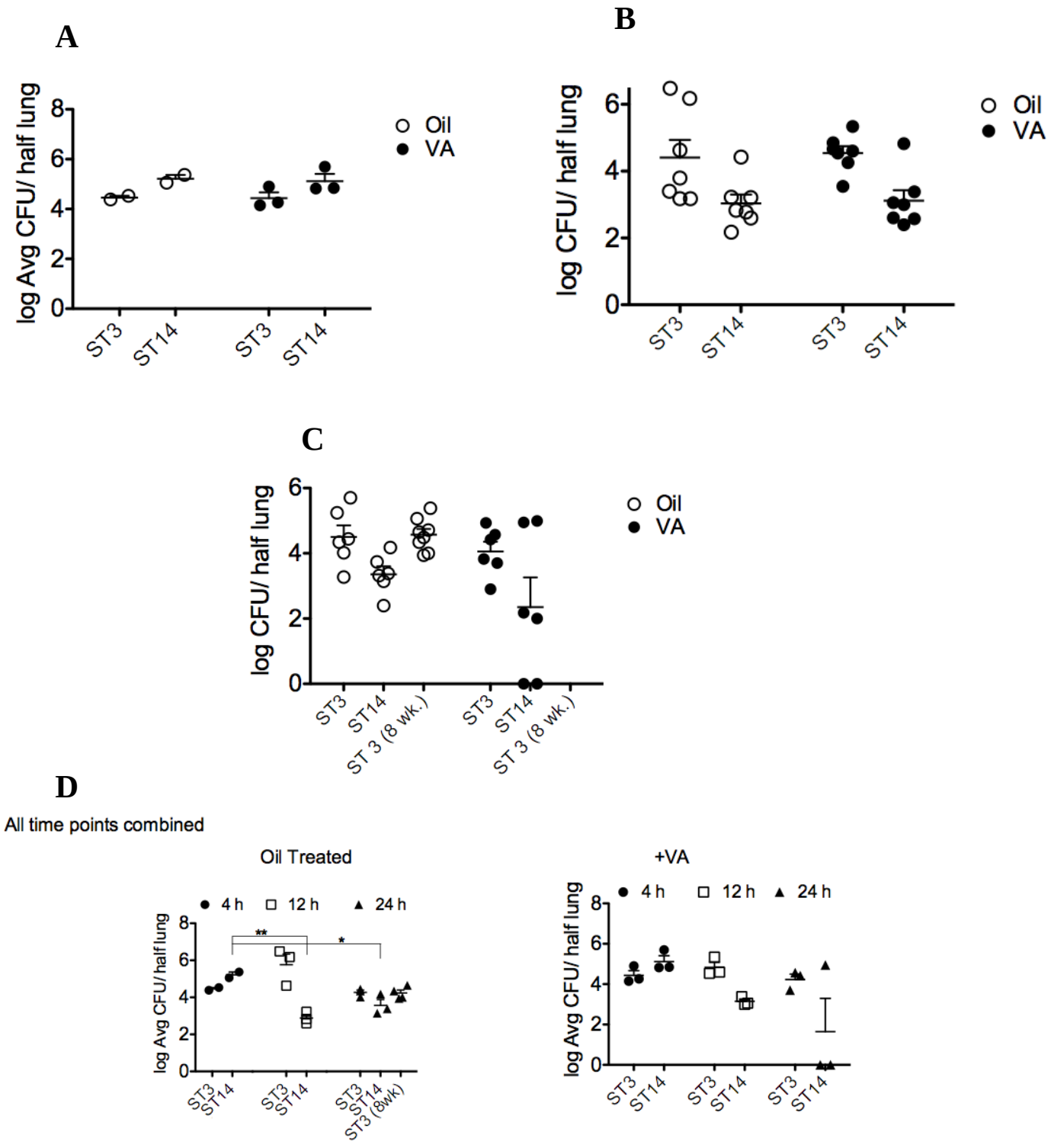

Figure 3: Bacterial recovery from the lung during the acute phase of pneumococcal pneumonia infection

Animals were dosed with VA or vehicle, and then infected with 1 x 10^5 CFUs *S. pneumoniae* ST3 or 1 x 10^7 CFUs *S. pneumoniae* ST14. Animals were euthanized at 4, 14, and 24 h. p.i., and the lungs were collected. Lung homogenates were serially diluted and plated overnight to determine bacterial load. Log CFU values ± SD are shown. Each plot represents one animal. An asterisk is used to denote statistical significance as determined by a two−way ANOVA with Bonferroni's post−hoc test. $P < 0.05$ was considered significant. Data shown is from one (A) or 3 *in vivo* experiments (B, C, D). Data is representative of lung bacterial recovery at 4 h (A), 12 h (B), and 24 h (C) p.i. Panel D illustrates all experiments combined (n = 12−15 animals per group).

Flow cytometry preparation and gating

Lung cells were stained with 0.1 μg of fluorochrome−labeled antibody prior to fixation with 1% paraformaldehyde. The addition of paraformaldehyde effectively killed the cells, but was used to preserve cell integrity. Prior to sample analysis, cellular debris and undesirable cell types must be excluded from analysis to ensure an appropriate population was analyzed. Therefore, unstained cells were run on the cytometer, and the lymphocyte population was chosen based on size and complexity (i.e., forward scatter and side scatter, respectively). This is gate R1, and represents a presumably live lymphocyte population. A representative R1 gate is shown in Figure 4. Only these cells were used for further analysis of CD marker expression. Additionally, compensation was performed on each single−stained sample to ensure that spectral overlap was not present on samples stained with multiple antibodies. The unstained and single−stained samples were pooled from both control and infected samples to ensure a representative population of cells.

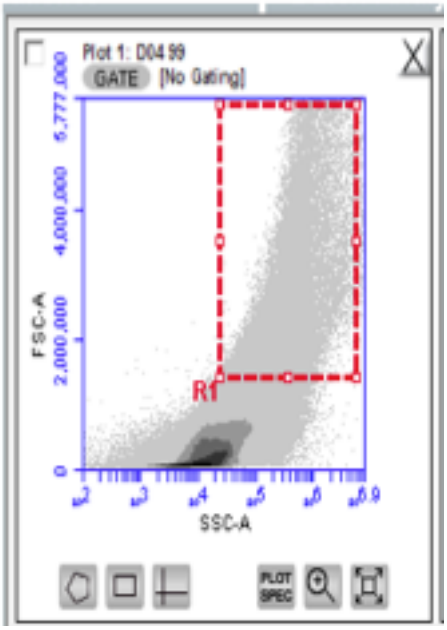

Figure 4: A forward scatter (FSC)/side scatter (SSC) plot of 2 x 10^5 unstained lung cells

The R1 gate represents the live population of lymphocytes used for further CD marker analysis. Anything outside the R1 gate is considered cellular debris or undesirable cell populations (i.e., epithelial cells, broken cells, etc.).

Effect of VA supplementation on myeloid cell populations

Animals infected with *S. pneumoniae* ST3 or ST14 were dosed with 1550 μg of retinyl palmitate in 10 μl of oil one time per day 2 days immediately before inoculation (pnd 12 and 13). Pups were sacrificed at 4, 12, and 24 h p.i. The gating for myeloid populations is described in the figure legends corresponding to each population (i.e., macrophages [mϕ], DCs, and myeloid cells [monocytes, basophils, eosinophils, neutrophils, mast cells, macrophages, and NK cells]). Figure 5 demonstrates mϕ infiltration to the lung at 4, 12, and 24 h p.i.

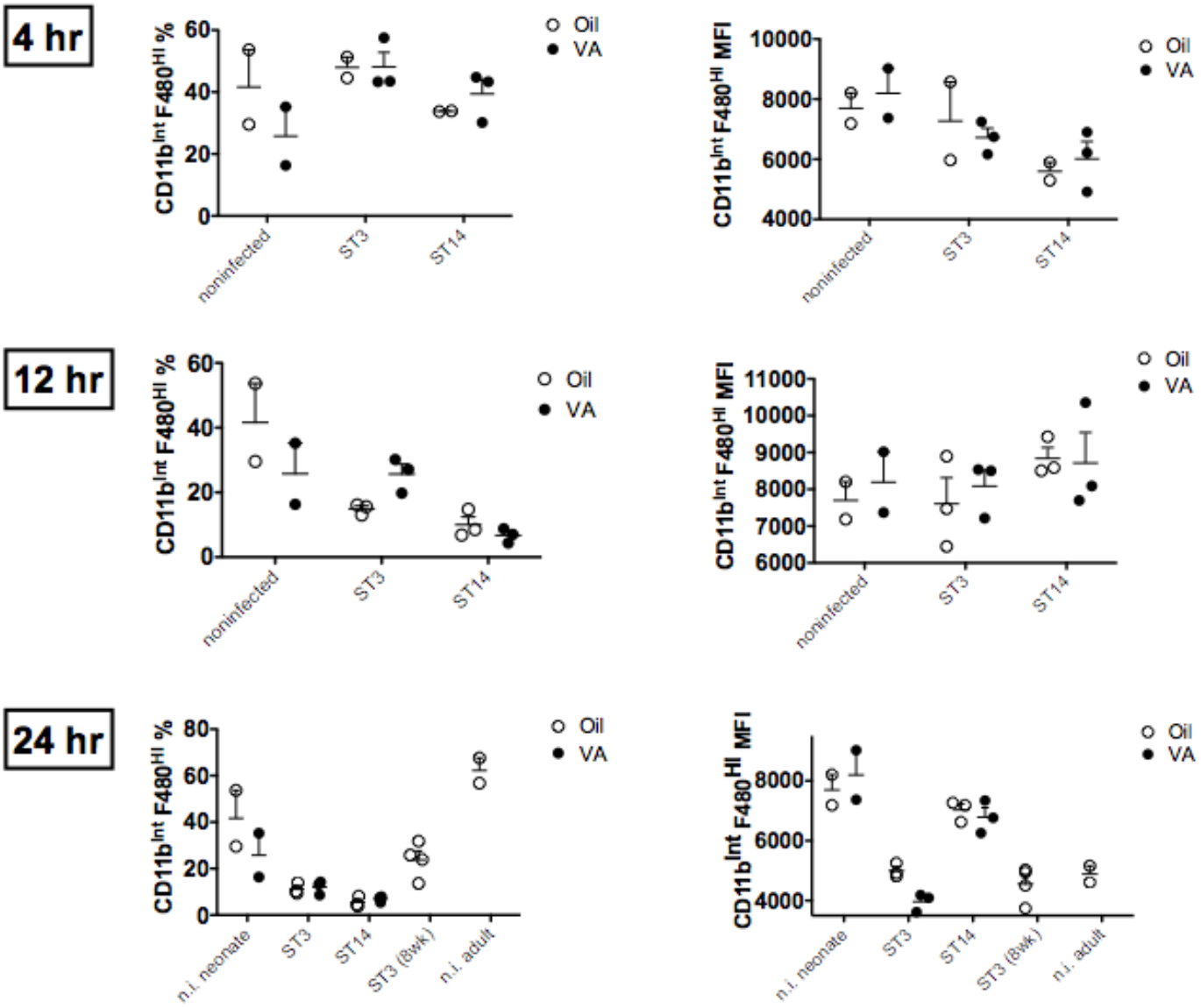

Figure 5: Mϕ populations at 4, 12, and 24 h p.i.

Two x 10^5 lung cells from *S. pneumoniae* ST3− or ST14− infected animals (neonates pnd 14 and 8. wk adult females), treated with oil or retinyl palmitate supplement, were stained with 0.1 μg of CD45, CD11c, CD11b, and F4/80. R1 gate was chosen to include presumably live lymphocyte populations. All further gating and analysis was done within the R1 gate. Single−stain, pooled samples were gated on % positive stained for each antibody. CD45+ staining was used as a marker for lymphocyte populations. Mϕ populations were analyzed within the M3 gate (i.e, from the % CD45+ cells). CD11b+/CD45+ populations represent the myeloid population. Each plot represents a single animal from one *in vivo* experiment ± SD. Data was analyzed for significance between the treatment groups (i.e., VA or vehicle−treated) by two−way ANOVA with Bonferroni's post−hoc test. $P < 0.05$ (denoted by 1 asterisk) was considered significant.

VA treatment had no effect on mϕ infiltration at 4 h p.i. However, retinyl palmitate supplementation in neonates infected with ST3 appeared to increase the mϕ population in the lung at 12 h p.i. Conversely, VA supplementation in neonates infected with ST3 decreased the mϕ mean fluorescence intensity (MFI), or the amount of CD markers present on each cell, in the lung at 24 h p.i (Figure 5). Note, however, that non−infected controls and adult mice infected with ST3 (24 h.) were omitted from analysis in order to strictly compare the effect of VA supplementation on cellular infiltration during an acute pneumococcal pneumonia infection in neonatal mice. Adults were included as a reference value. Additionally note that a difference in mϕ infiltration at all time points was observed between serotypes, but the difference was not significant as determined by Bonferroni's post−hoc analysis. Briefly, there is a dramatic decrease in mϕ populations from 4 to 12 h p.i. with both ST3 and ST14. An even larger decrease is observed in mϕ populations from 4 to 24 h p.i. with both ST3 and ST14. Similarly, MFI gradually decreases from 4 to 24 h p.i.

CD11b+ populations were also analyzed in the lung of neonatal and adult mice infected with ST3 or ST14, and supplemented with retinyl palmitate or vehicle (Figure 6). CD11b+ cells represent granulocytes (eosinophils, basophils, mast cells, and neutrophils), monocytes, macrophages, and NK cells. VA supplementation had no effect on CD11b cell populations or MFI. However, there was a distinct observable trend between serotypes. Specifically, ST 3−infected animals showed an increase in CD11b+ cell numbers and MFI from4 to 12 h p.i and 12 to 24 hours p.i. ST 14−infected animals also displayed an increase in MFI from 4 to 12 h p.i. and 4 to 24 h p.i. Noninfected controls and adults (8 wk) were excluded from the statistical analysis.

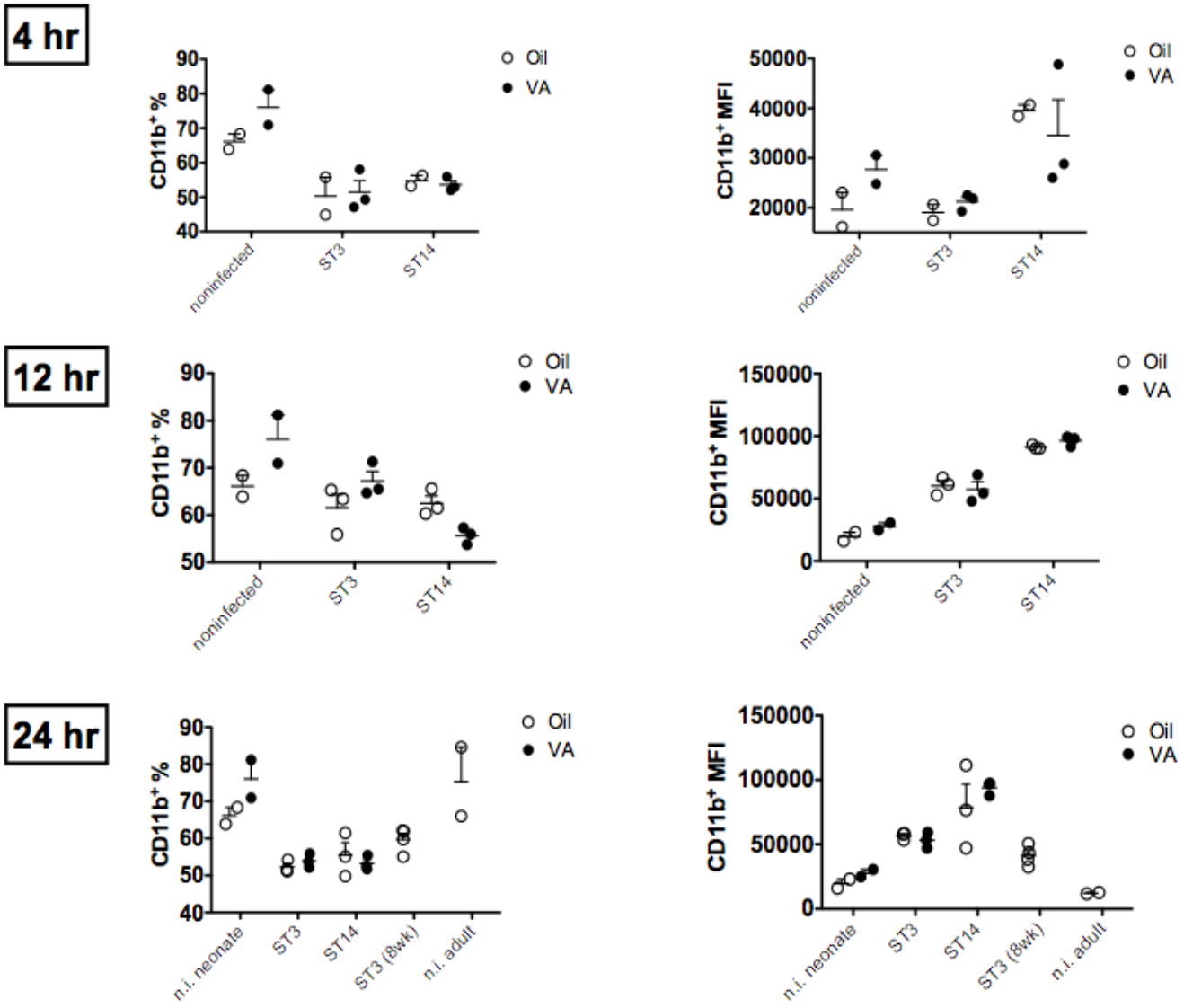

Figure 6: CD11b+ populations at 4, 12, and 24 h p.i.

Two x 10^5 lung cells from *S. pneumoniae* ST3− or ST14− infected animals (neonates pnd 14 and 8. wk adult females), treated with oil or retinyl palmitate supplement, were stained with 0.1 μg of CD11b, CD11c, Gr−1, and F4/80. R1 gate was chosen to include presumably live lymphocyte populations. All further gating and analysis was done within the R1 gate. Single−stain, pooled samples were gated on % positive stained for each antibody. CD45+ staining was used as a marker for lymphocyte populations. CD11b+ populations were analyzed within the M3 gate (i.e, from the % CD45+ cells). CD45+/CD11b populations represent the DC population. Each plot represents a single animal from one *in vivo* experiment ± SD. Data was analyzed for significance between the treatment groups (i.e., VA or vehicle−treated) by two−way ANOVA with Bonferroni's post−hoc test.

Moreover, CD11c+ DC populations were analyzed in the lung. Retinyl palmitate supplementation had no effect on DC population percent or MFI at any of the time points (Figure 7). Non−infected controls and adult mice infected with ST3 (24 h) were omitted from the statistical analysis in order to exclusively examine the effect of VA supplementation on DC populations in the lung of infected pups (pnd 14). Adult female mice (8 wk) were included as a reference value. An observable kinetic trend in MFI was observed between the different time points. That is, CD11c+ MFI was lowest at 4 h p.i, and gradually increased at 12 and 24 h p.i for both serotypes.

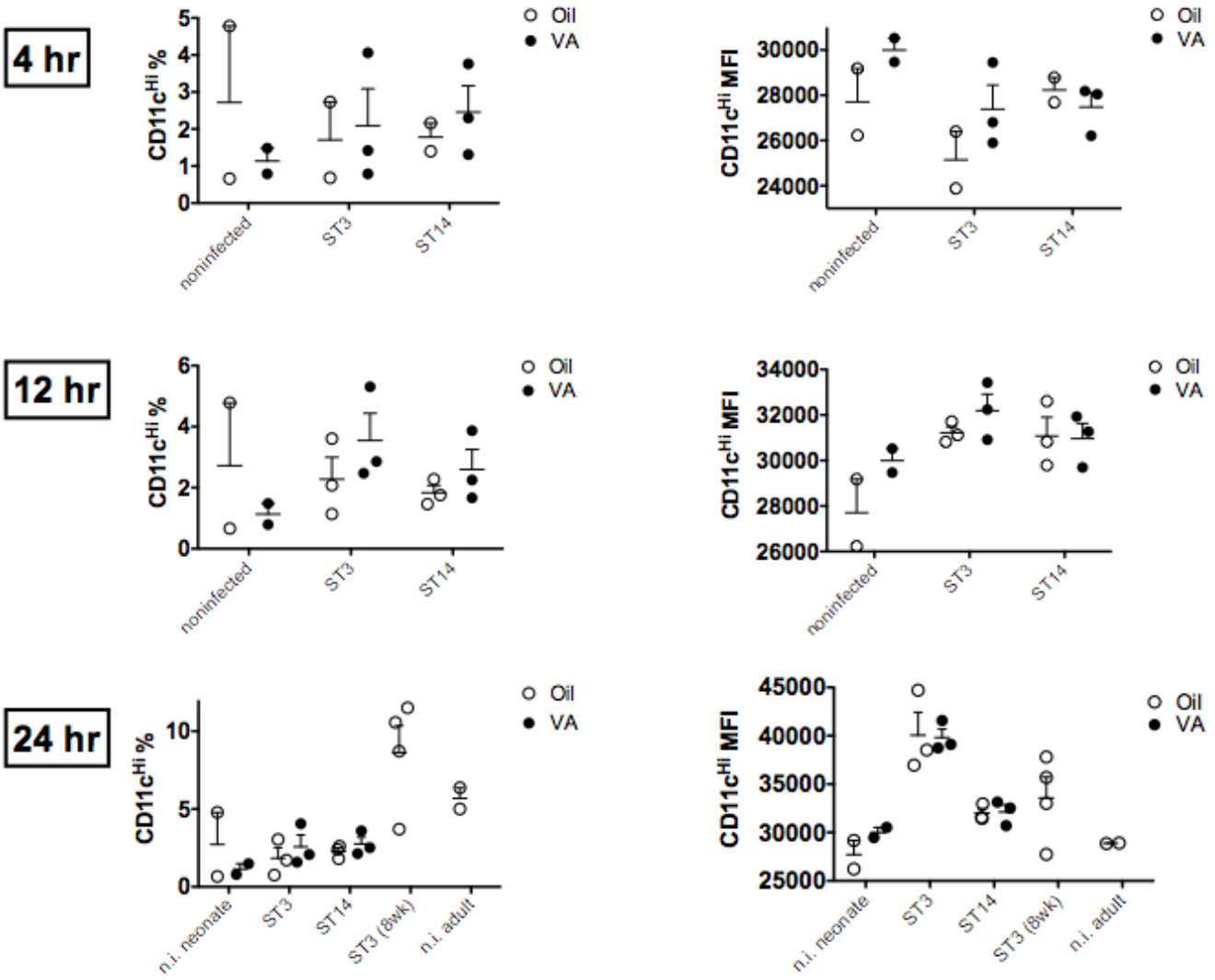

Figure 7: DC populations at 4, 12, and 24 h p.i.

Two x 10^5 lung cells from *S. pneumoniae* ST3− or ST14− infected animals (neonates pnd 14 and 8. wk adult females), treated with oil or retinyl palmitate supplement, were stained with 0.1 µg of CD11b, CD11c, Gr−1, and F4/80. R1 gate was chosen to include presumably live lymphocyte populations. All further gating an analysis was done within the R1 gate. Single−stain, pooled samples were gated on % positive stained for each antibody. CD45+ staining was used as a marker for lymphocyte populations. Gr−1+ populations were analyzed within the M3 gate (i.e, from the % CD45+ cells). CD11b+/CD11c^{Hi} populations represent the DC population. Each plot represents a single animal from three combined *in vivo* experiments ± SD. Data was analyzed for significance between the treatment groups (i.e., VA or vehicle−treated) by two−way ANOVA with Bonferroni's post−hoc test. $P < 0.05$ (denoted by 1 asterisk) was considered significant.

Finally, Gr1+ granulocytes were analyzed in the lung of control and infected mice at 12 and 24 h p.i (Figure 8). Please note that we omitted the 4 h time point from two later experiments, and combined the latter time points (12, 24 h) with the first experiment. Retinyl palmitate had no effect on granulocyte number or MFI, but there was a distinct observable trend between the serotypes. That is, granulocyte populations were increased in ST3− infected mice compared to mice inoculated with ST14, but the MFI was much higher in ST14−infected mice compared to ST3−infected mice (Figure 8A and 8B). This trend was irrespective of treatment and observed at both 12 and 24 h p.i. Additionally, non−infected controls and adult females infected with ST3 (24 h) were excluded from the statistical analysis in order to analyze the interaction between VA supplementation and granulocyte populations in the lung.

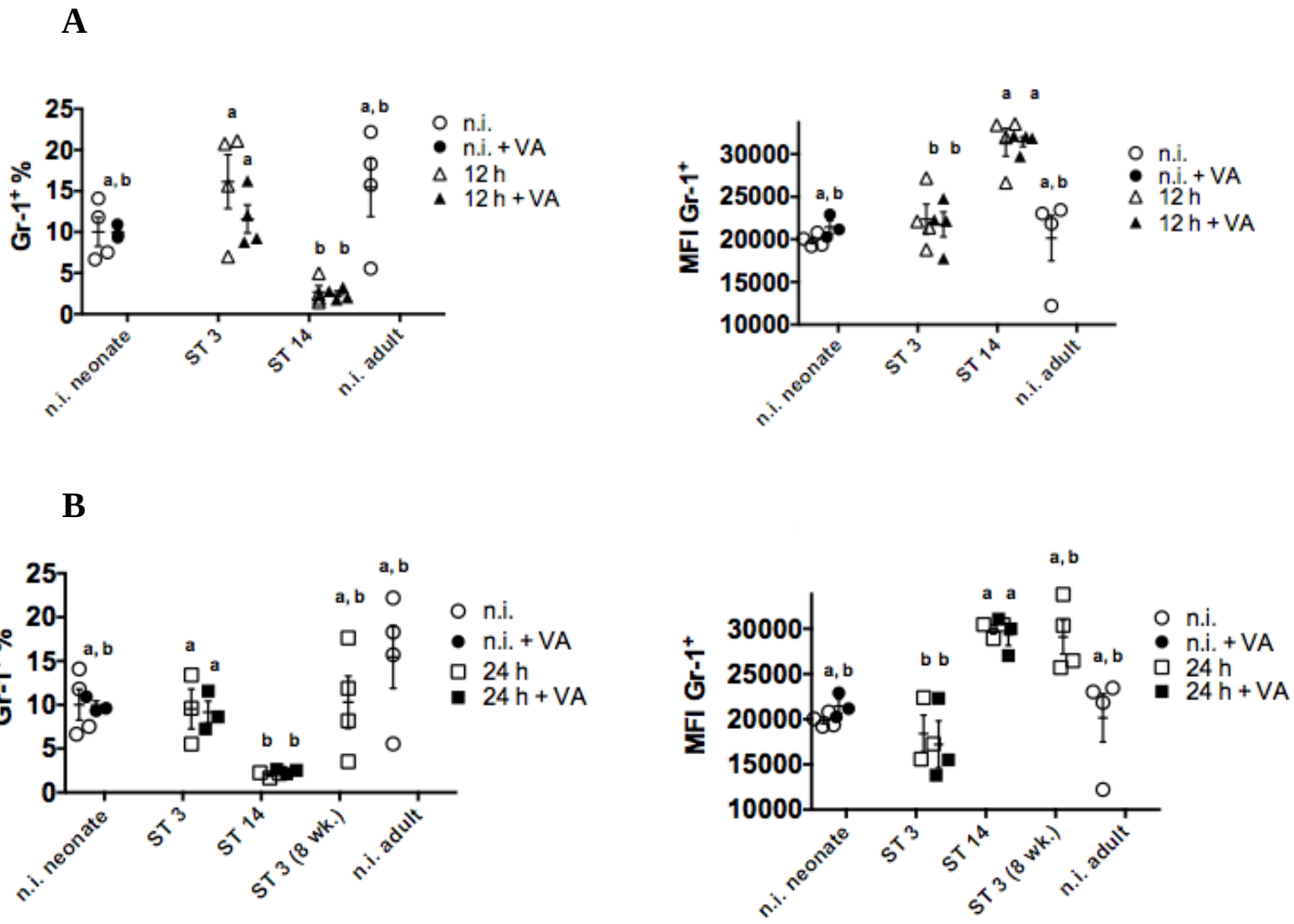

Figure 8: Gr−1+ populations at 12 and 24 h p.i.

Two x 10^5 lung cells from *S. pneumoniae* ST3− or ST14− infected animals (neonates pnd 14 and 8. wk adult females), treated with oil or retinyl palmitate supplement, were stained with 0.1 µg of Gr−1, CD11c, CD11b, and F4/80. R1 gate was chosen to include presumably live lymphocyte populations. All further gating an analysis was done within the R1 gate. Single−stain, pooled samples were gated on % positive stained for each antibody. CD45+ staining was used as a marker for lymphocyte populations. Granulocyte populations were analyzed within the M3 gate (i.e, from the % CD45+ cells). CD45+/Gr−1+ populations represent the granulocyte population. Each plot represents a single animal from three combined *in vivo* experiments ± SD. Data was analyzed for significance between the treatment groups (i.e., VA or vehicle−treated) by two−way ANOVA with Bonferroni's post−hoc test. $P < 0.05$ (denoted by a, b) was considered significant. A) Gr−1+ % of population and MFI at 12 h p.i. B) Gr−1% of population and MFI at 24 h p.i.

Effect of VA supplementation on lymphocyte populations

First, the effect of VA supplementation on B cell populations was analyzed. We first used B220 as a marker of B cells, and CD19 was used as a B cell marker in later experiments. Interestingly, VA supplementation to non−infected animals dramatically increased the MFI of B cells compared to oil−dosed controls, but animals infected with *S. pneumoniae* ST3 or ST14 did not display an increase in MFI or B cell populations with retinyl palmitate supplementation at any time points (Figure 9). However, there was an observable trend between serotypes. The percent of B cells present in the lung increased from 4 to 12 h p.i, and from 4 to 24 h p.i in animals inoculated with ST3 and dosed with oil. Additionally, B cell percent in the lung increased from 12 to 24 h p.i in neonates inoculated with ST3 and dosed with VA. Non−infected controls and adults (24 h) were excluded from the statistical analysis.

Moreover, CD19 was also used as a B cell marker in later experiments (Figure 10). We observed an inverse relationship between CD19+ populations and CD19 expression (MFI). Specifically, animals infected with ST3 had a much larger CD19+ population compared to animals infected with ST14, but the MFI was greater in animals infected with ST14 compared to ST3 (Figure 10A and 10B). However, the increase in MFI was not considered significant as determined by Bonferroni's post−hoc analysis. Non−infected controls and adult mice (24 h) were excluded from the statistical analysis. Adult mice were included for a reference value.

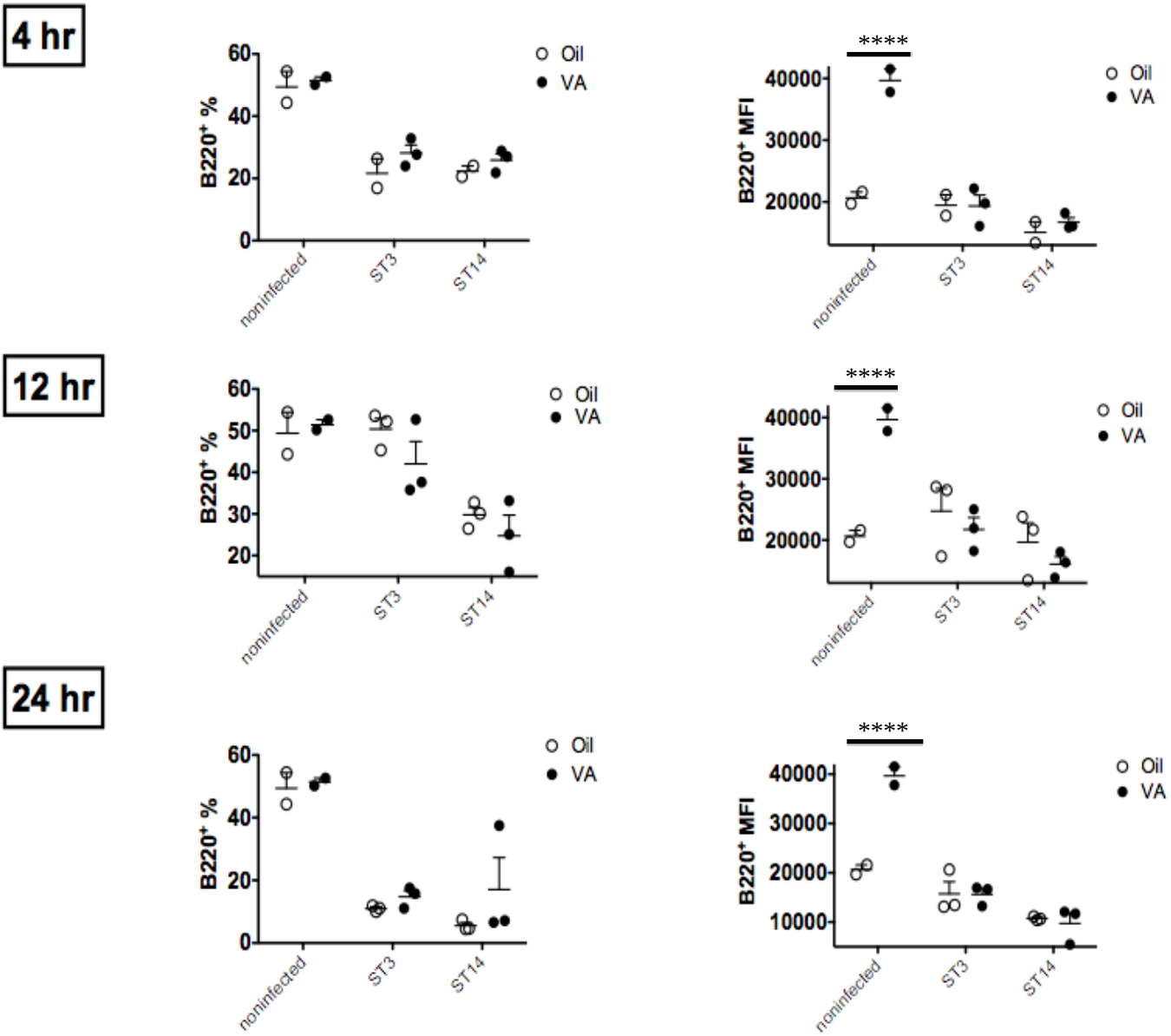

Figure 9: B220+ populations at 4, 12, and 24 h p.i.

Two x 10^5 lung cells from *S. pneumoniae* ST3− or ST14− infected animals (neonates pnd 14 and 8. wk adult females), treated with oil or retinyl palmitate supplement, were stained with 0.1 µg of Gr−1, CD45, B220, and CD3. R1 gate was chosen to include presumably live lymphocyte populations. All further gating an analysis was done within the R1 gate. Single−stain, pooled samples were gated on % positive stained for each antibody. CD45+ staining was used as a marker for lymphocyte populations. Granulocyte populations were analyzed within the M3 gate (i.e, from the % CD45+ cells). CD45+/B220+ populations represent the B cell population. Each plot represents a single animal from one *in vivo* experiment ± SD. Data was analyzed for significance between the treatment groups (i.e., VA or vehicle−treated) by two−way ANOVA with Bonferroni's post−hoc test. $P < 0.05$ (denoted by an asterisk) was considered significant.

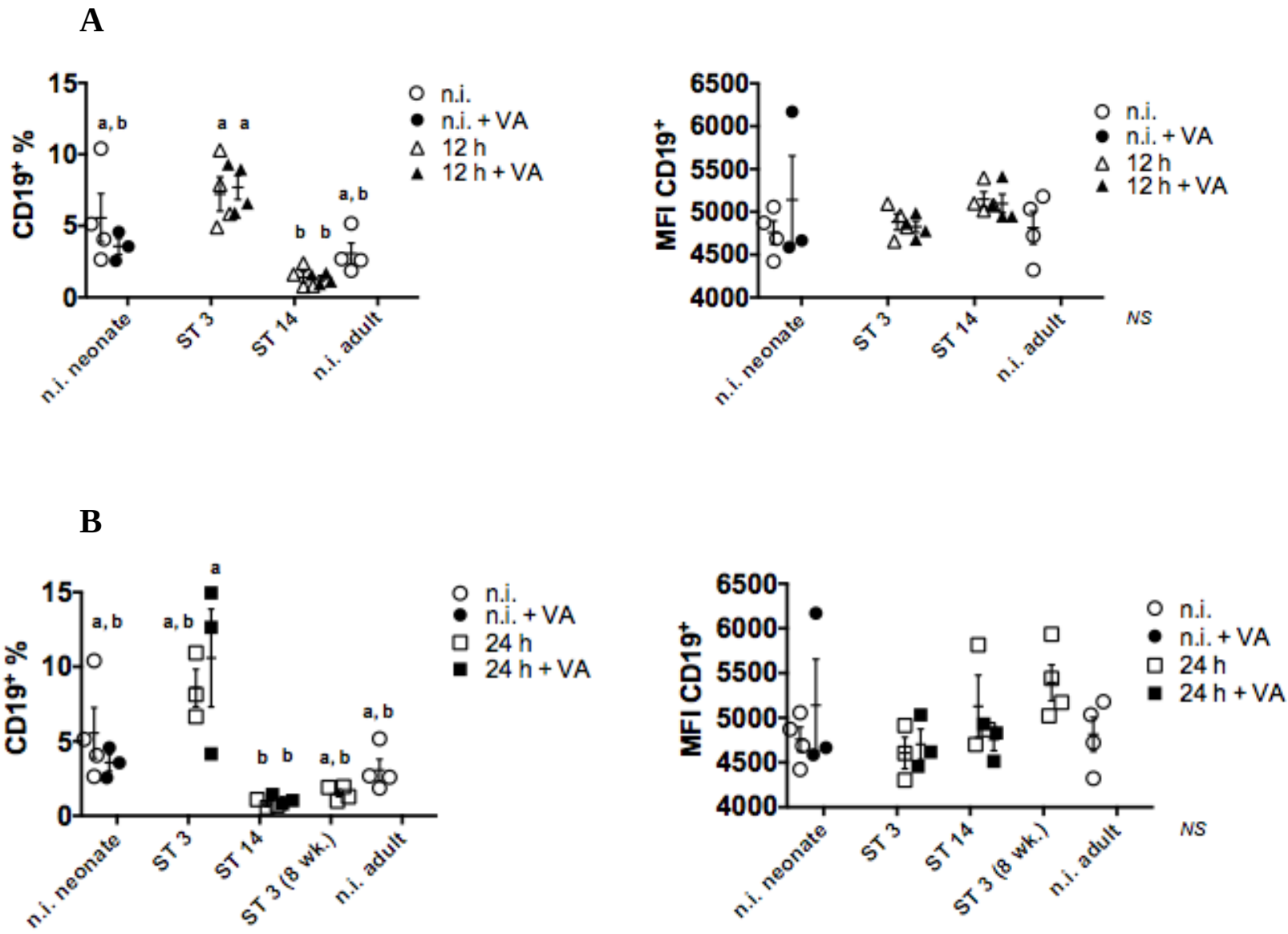

Figure 10: CD19+ populations at 12 and 24 h p.i.

Two x 10^5 lung cells from *S. pneumoniae* ST3− or ST14− infected animals (neonates pnd 14 and 8. wk adult females), treated with oil or retinyl palmitate supplement, were stained with 0.1 µg of Gr−1, CD45, CD19, and CD3. R1 gate was chosen to include presumably live lymphocyte populations. All further gating an analysis was done within the R1 gate. Single−stain, pooled samples were gated on % positive stained for each antibody. CD45+ staining was used as a marker for lymphocyte populations. Granulocyte populations were analyzed within the M3 gate (i.e, from the % CD45+ cells). CD45+/CD19+ populations represent the B cell population. Each plot represents a single animal from 2 combined *in vivo* experiments ±SD . Data was analyzed for significance between the treatment groups (i.e., VA or vehicle−treated) by two−way ANOVA with Bonferroni's post−hoc test. $P < 0.05$ (denoted by a, b) was considered significant. A) CD19+ % of population and MFI at 12 h p.i. B) CD19+ % of population and MFO at 24 h p.i.

Finally, the proportion of T cells in the lung tissue was analyzed (Figure 11). CD3 is a T cell marker expressed on all T cell subsets, and was chosen to give a broad picture of T cell activity during an acute pneumococcal pneumonia infection in neonatal mice. Retinyl palmitate supplementation had no effect on CD3 population or MFI (Figure 10A and 10B). Nonetheless, there was a difference observed between infection with ST3 and ST14. Infection with *S. pneumoniae* ST3 produced a larger T cell population in the lung compared to ST14 infection at both 12 and 24 h p.i. Conversely, the MFI was significantly decreased during ST3 infection compared to ST14 at both 12 and 24 h p.i (Figure 10A and 10B). Adults and non−infected control neonates were excluded from the statistical analysis to exclusively analyze the interaction between retinyl palmitate supplementation and T cell populations.

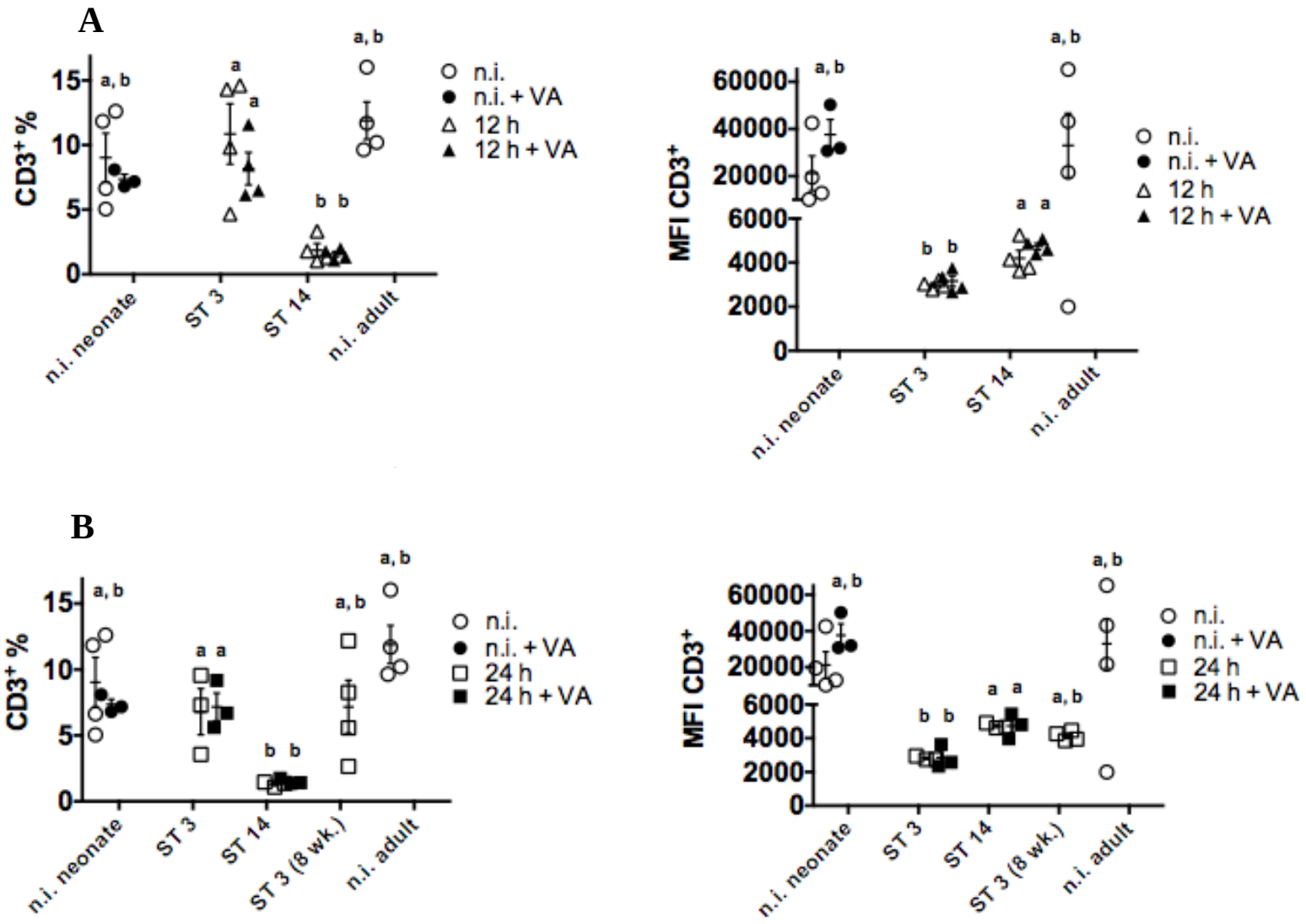

Figure 11: CD3+ populations at 12 and 24 h p.i.

Two x 10^5 lung cells from *S. pneumoniae* ST3− or ST14− infected animals (neonates pnd 14 and 8. wk adult females), treated with oil or retinyl palmitate supplement, were stained with 0.1 µg of Gr−1, CD45, CD19, and CD3. R1 gate was chosen to include presumably live lymphocyte populations. All further gating an analysis was done within the R1 gate. Single−stain, pooled samples were gated on % positive stained for each antibody. CD45+ staining was used as a marker for lymphocyte populations. Granulocyte populations were analyzed within the M3 gate (i.e, from the % CD45+ cells). CD45+/CD3+ populations represent the T cell population. Each plot represents a single animal from one *in vivo* experiment ± SD. Data was analyzed for significance between the treatment groups (i.e., VA or vehicle−treated) by two−way ANOVA with Bonferroni's post−hoc test. $P < 0.05$ (denoted by a, b) was considered significant. A) CD3+ % of population and MFI at 12 h p.i. B) CD3+ % of population and MFO at 24 h p.i.

In vivo neutrophil activity

Furthermore, a myeloperoxidase assay was performed to confirm the increase in neutrophil activity observed during infection with *S. pneumoniae* ST14. At 12 h p.i., animals infected with ST14 and treated with retinyl palmitate displayed a high increase in neutrophil activity compared to animals infected with ST3 and supplemented with VA (Figure 12). Additionally, a kinetic trend was observed over time. Neutrophil activity was lowest at 4 h p.i, and peaked at 12 h p.i., irrespective of treatment (Figure 12). Please note that adults infected with ST3 (24 h) were excluded from the statistical analysis to strictly examine neutrophil activity in animals infected with *S. pneumoniae* ST3 and ST14.

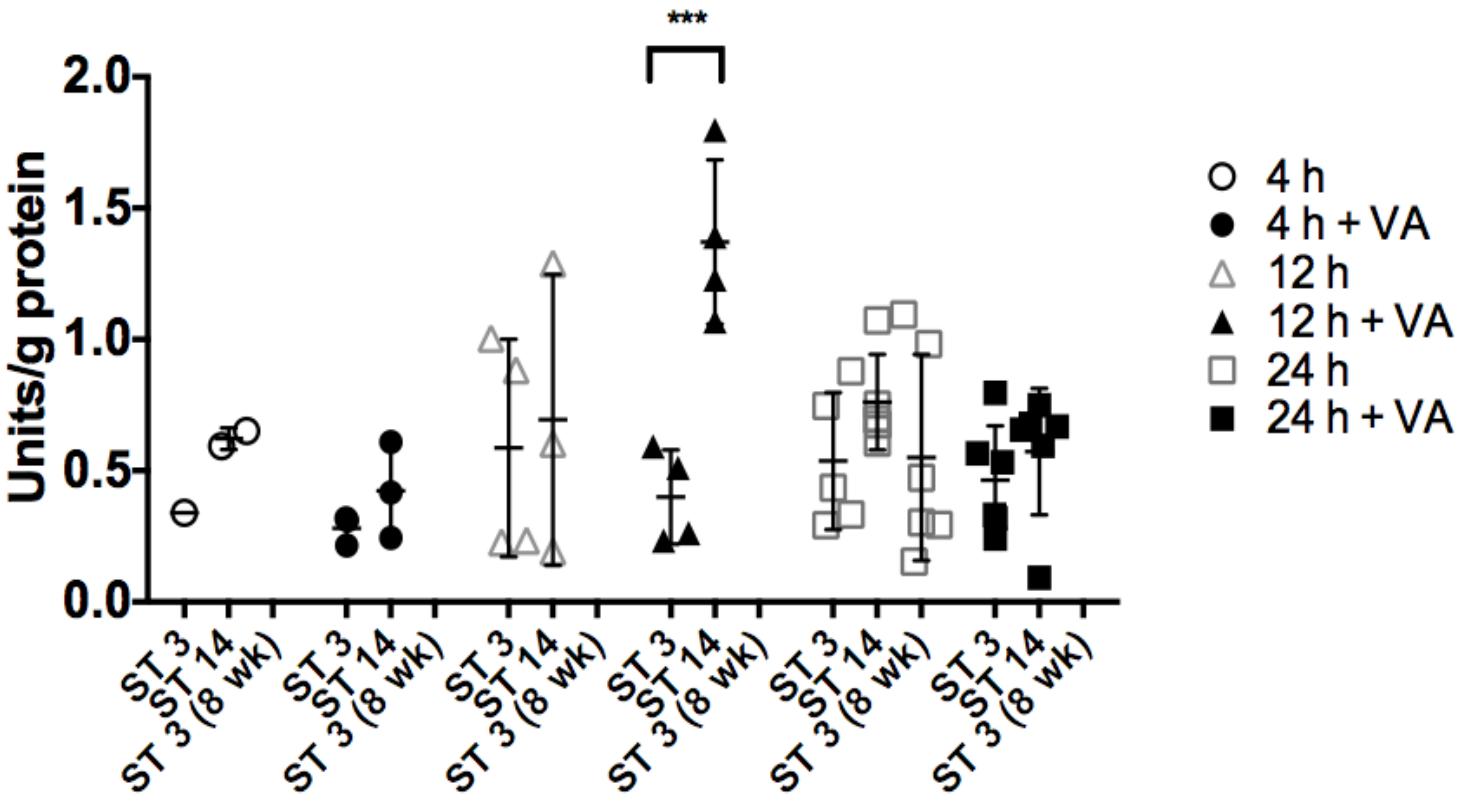

Figure 12: Neutrophil activity at 4, 12, and 24 h p.i.

The left lobe of the lung was homogenized in 1 ml 1x PBS, and subjected to freeze/thaw cycles (2x) and vigorous vortexing to extract the enzyme. Samples were then centrifuged at 5000 x g (6080 rpm in Beckman centrifuge) for 30 min at 4° C, and the supernatant was collected. In a 96 well plate, samples were 3−fold serially diluted in potassium phosphate buffer. Afterwards, *O*−dianisidine HCL solution (*o*−dianisidine HCL and 50 mM potassium phosphate buffer, 0.334 mg/ml) was added to the samples to achieve a final concentration of 0.167 mg/ml. Standard (commercial MPO, BD Biosciences) was 2−fold serially diluted to yield a standard curve. One percent hydrogen peroxide was added to the standard and samples to initiate the enzymatic reaction. After 30 s, samples were read on a plate reader at 450 nm. Specific activity was measured as units of enzyme activity per g of protein. The second dilution was used for analysis. Each plot represents a single animal from two combined *in vivo* experiments ± SD. Two−way ANOVA with Bonferroni's post−hoc analysis was used to determine the significance over time and with treatment. $P < 0.05$ was considered significant

Liver retinol (ROH) levels

Finally, ultra−performance liquid chromatography was used to assess the VA status of animals fed a VAM diet and supplemented with either retinyl palmitate or oil control. Liver ROH levels were significantly increased ($P < 005$) in ST3− and ST14−infected mice supplemented with retinyl palmitate compared to animals supplemented with vehicle (canola oil) (Figure 13). However, the pups did not have a vitamin A marginal status, as expected. Rather, pups supplemented with oil contained VA adequate (VAA) liver retinol concentrations, and the pups supplemented with retinyl palmitate contained even greater VA concentrations. Thus, the next set of experiments was designed to solely elucidate the differences in pneumococcal colonization and cellular infiltration in neonatal mice infected with ST3 and ST14. Please note that controls (control, control+ VA) were excluded from the statistical analysis to focus on the effect of VA supplementation on liver ROH concentrations in ST3− and ST14−infected mice. Controls were shown as a reference value.

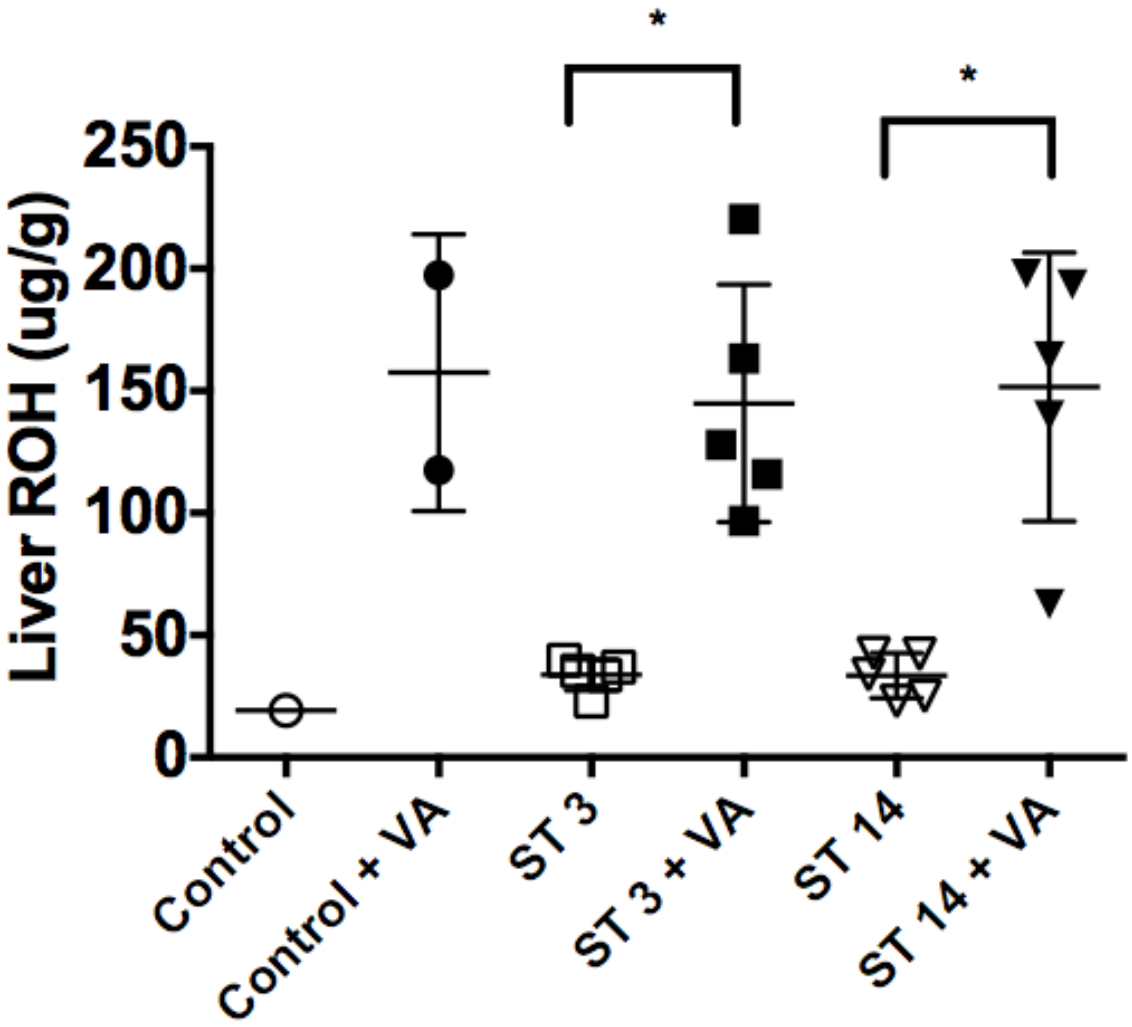

Figure 13: Neonatal liver ROH concentration

Dams (8 wks. old) were fed a VAM diet through gestation, birth, and lactation (until pups were pnd 14). Pups were supplemented with 1550 μg retinyl palmitate in 10 μl oil or vehicle (10 μl canola oil) 1 time per day for 2 days before inoculation with ST3 or ST14 (pnd 12 and 13). Animals were sacrificed 24 h p.i. and livers were flash frozen in liquid nitrogen, and stored at −80° C. For UPLC analysis, lung tissue was weighed, homogenized and subsequently extracted in a chloroform:methanol (2:1, v/v) solution overnight. Trimethylmethoxyphenyl−retinol was used as the internal standard, and added to portions of total lipid extracts. Samples were then dried and reconstituted in chloroform:methanol (1:1) solution for UPLC analysis. Approximately 7 μL sample volume was injected onto a C−18 reverse−phase UPLC column, and eluted with 90:10 methanol−water and eventually 100% methanol (gradient mobile phase). The eluted sample was analyzed at 325 nm. Each plot represents a single animal from one *in vivo* experiment ± SD. Data was analyzed with one−way ANOVA with Tukey's multiple comparisons post−hoc analysis. $P < 0.05$ was considered significant (denoted with one asterisk).

Part 2: A comparison of *S. pneumoniae* ST 3 and ST 14 infection in neonatal mice

Experimental Design

All animals were fed a standard chow diet throughout the duration of the experiments. The experimental design is illustrated in Figure 14.

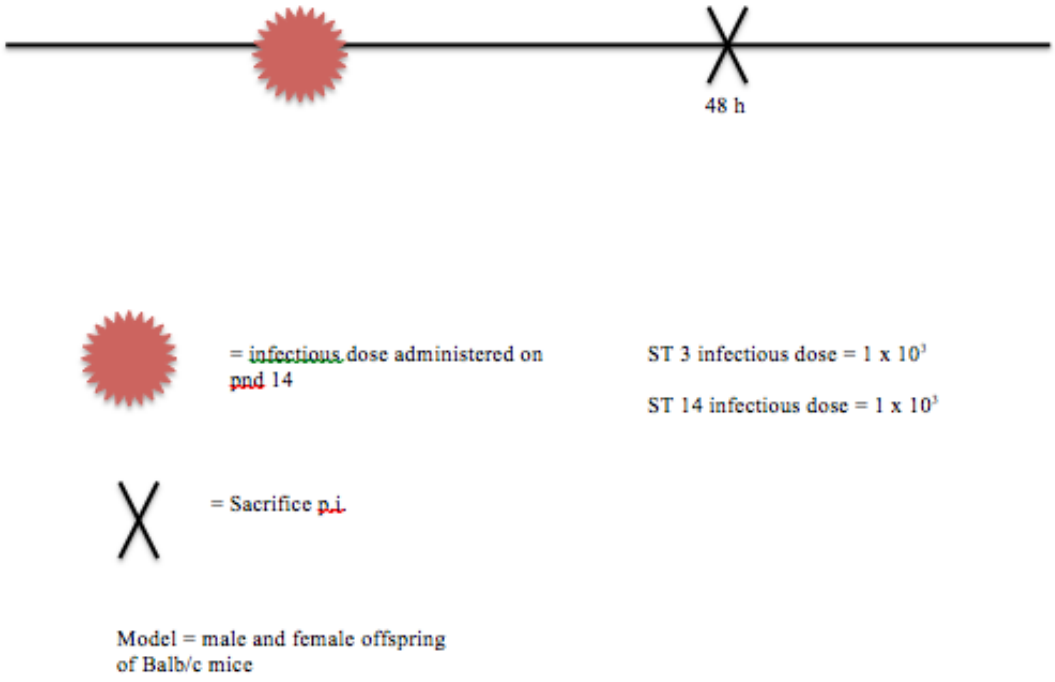

Figure 14: Experimental design for ST3 vs. ST14 comparison studies (experiment 1)

Lung and blood bacterial load during acute phase pneumococcal pneumonia

After inoculation, mice were sacrificed at 48 h p.i and a small portion of the right lobe of the lung was homogenized in an equal−volume amount of PBS (i.e., 1 μg = 1 μl). Briefly, the lung homogenates were serially diluted, and grown on agar plates O/N to determine lung bacterial loads. Only one mouse infected with ST14 produced colonies on the plates (data not shown). Otherwise, the plates were void of bacterial colonies. Additionally, 10 μl of whole blood was plated on blood agar plates and grown O/N. No animals displayed signs of bacteremia (data not shown).

Flow cytometry−myeloid cell populations

Animals were inoculated with 1 x 10^3 CFUs of *S. pneumoniae* ST3 or ST14 on pnd 14. Animals were sacrificed 48 h p.i and analyzed for changes in granulocyte and macrophage cell populations. Pups infected with ST3 or ST14 showed no significant difference in granulocyte population relative to control, or between the serotypes (Figure 15A). Interestingly, mϕ populations were significantly increased in control neonates compared to neonates infected with ST3 or ST14 (Figure 15B).

Flow cytometry−NK cell populations

Animals were inoculated with 1 x 10^3 CFUs of *S. pneumoniae* ST3 or ST14 on pnd 14, and sacrificed at 48 h p.i. to analyze changes in NK and NK T cell populations in the lung. The percentage of NK or NK T cells did not significant increase relative to control, or between the serotypes (Figure 16A and 16B, respectively).

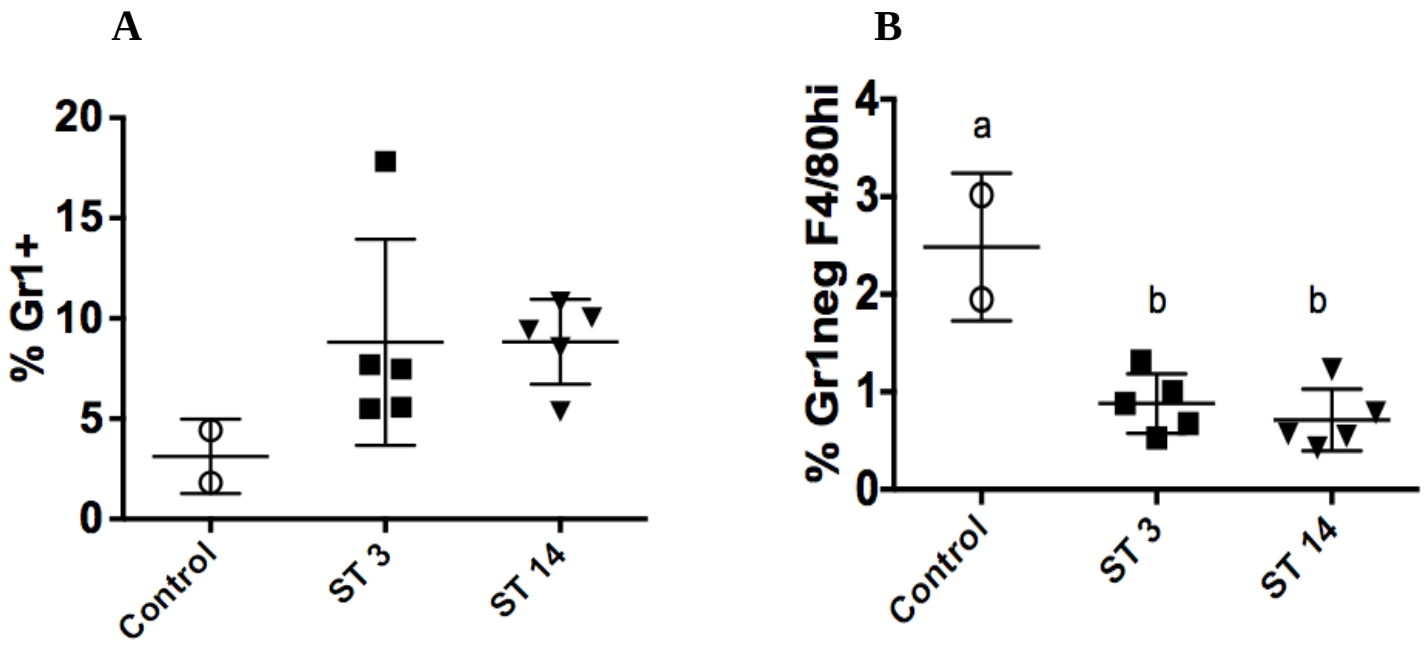

Figure 15: Myeloid cell populations at 48 h p.i.

Two x 10^5 lung cells from *S. pneumoniae* ST3− or ST14− infected animals (neonates pnd 14), were stained with 0.1 µg of Gr−1, CD11b, F4/80, and CD11c. R1 gate was chosen to include presumably live lymphocyte populations. Each plot represents a single animal from one *in vivo* experiment ± SD. Data was analyzed for significance between the serotypes by one−way ANOVA with Tukey's post−hoc test. $P < 0.05$ (denoted by a, b) was considered significant. A) CD11b+/Gr−1+ populations represent the granulocyte population. B) Within the CD11b+/Gr−1+ gate, the % of cells Gr−1−/F4/80^{Hi} represent the macrophage population.

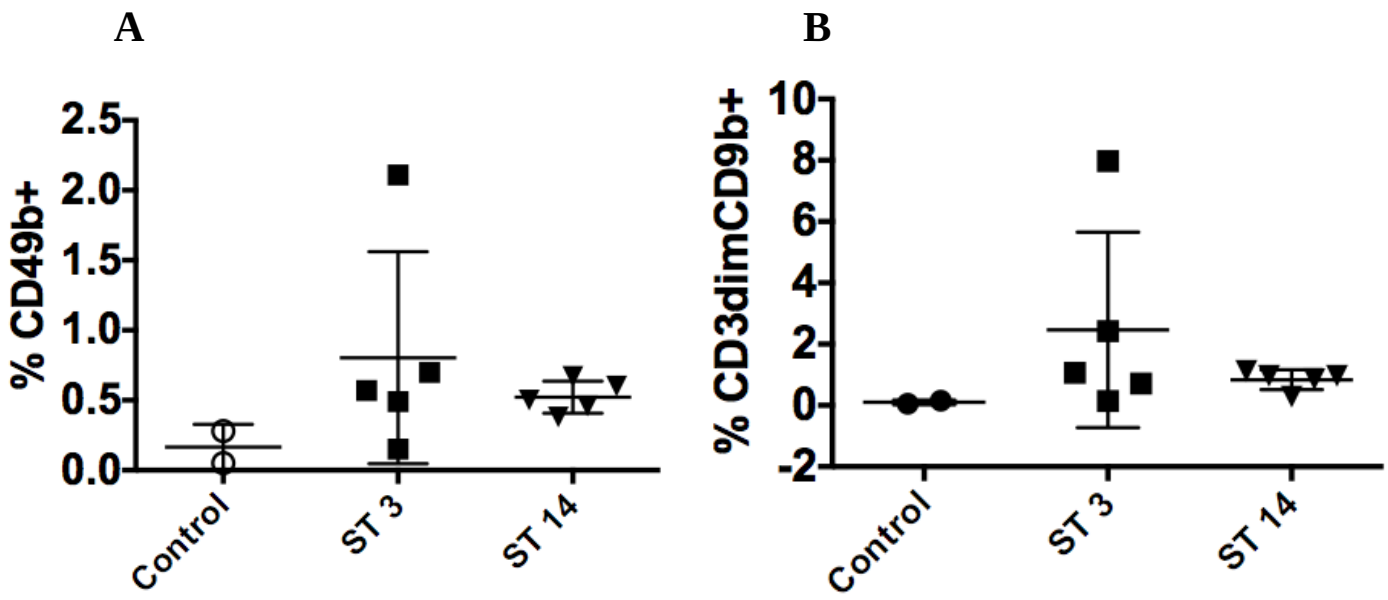

Figure 16: NK cell populations at 48 h p.i.

Two x 10^5 lung cells from *S. pneumoniae* ST3− or ST14− infected animals (neonates pnd 14), were stained with 0.1 µg of CD27, CD11b, CD49b, and CD3. R1 gate was chosen to include presumably live lymphocyte populations. Each plot represents a single animal from one *in vivo* experiment ± SD. Data was analyzed for significance between the serotypes by one−way ANOVA with Tukey's post−hoc test. A) Within the $CD11b^{Int}$ gate, CD49b+/CD27+ populations represent the NK cell population. B) Of the % of cells CD49b+/CD27+, cells that were CD3 dim represent the NK T cell population.

Since CFUs were not present in the lung or blood of neonates infected with 1 x 10^3 CFUs of *S. pneumoniae* ST3 or ST14, we decided to increase the inoculating dose of both serotypes. Figure 17 (below) displays the experimental design.

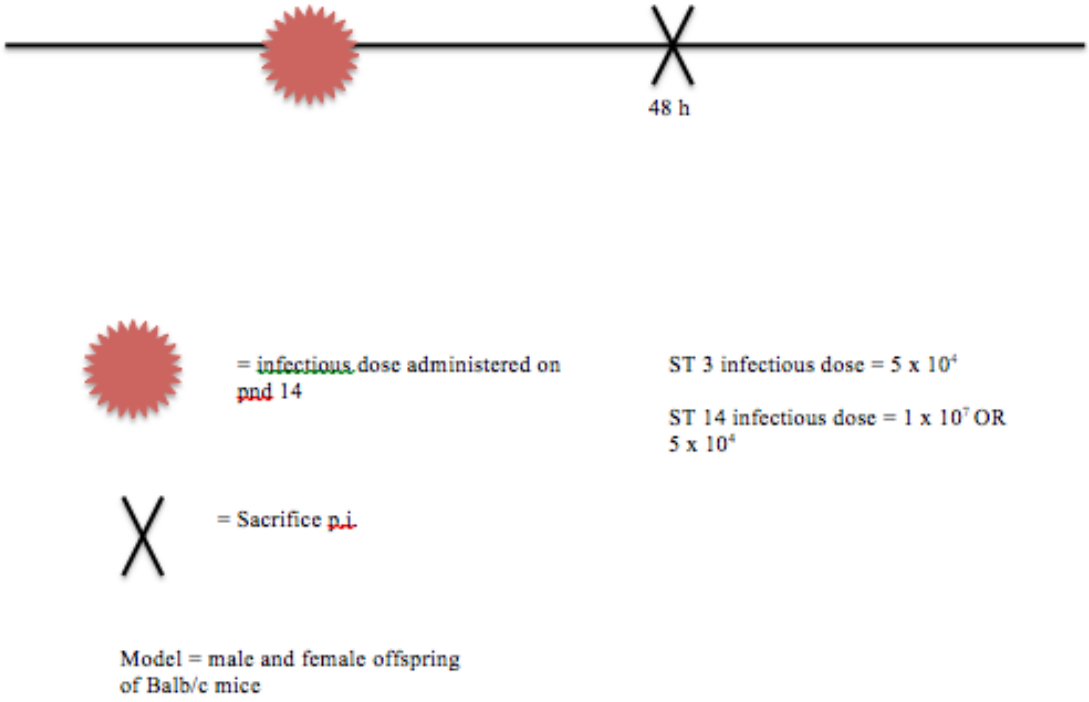

Figure 17: ST3 vs. ST14 experimental design (experiment 2)

Lung and blood bacterial load during acute phase pneumococcal pneumonia

Animals were infected with 5 x 10^4 CFUs *S. pneumoniae* ST3 or 1 x 10^7 or 5 x 10^4 CFUs *S. pneumoniae* ST14. Animals were euthanized at 24 h p.i to determine lung and blood bacterial load. No animals showed signs of bacteremia, as determined by whole blood CFU analysis (data not shown). However, pups infected with 5 x 10^4 CFUs of ST3 had significantly greater bacterial loads in the lung compared to animals inoculated with 5 x 10^4 CFUs ST14 (Figure 18). Interestingly, pups infected with the higher dose of ST14 did not contain higher bacterial counts in the lung (Figure 18).

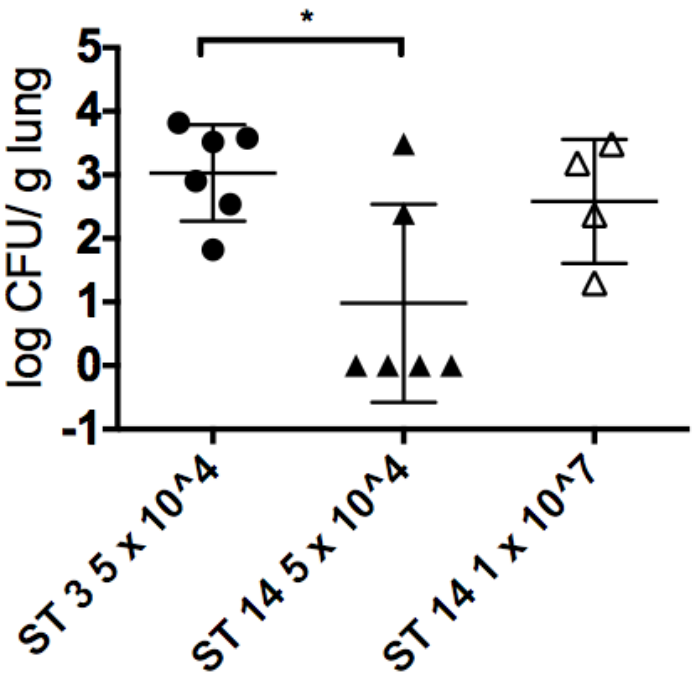

Figure 18: Bacterial recovery from the lung during the acute phase of pneumococcal pneumonia infection

Neonates (pnd 14) were infected with 5 x 10^4 CFUs *S. pneumoniae* ST3, 1 x 10^7 or 5 x 10^4 CFUs *S. pneumoniae* ST14. Animals were euthanized at 48 h. p.i., and the lungs were collected. Lung homogenates were serially diluted and plated overnight to determine bacterial load. Log CFU values ±SD are shown. Each plot represents one animal from one *in vivo* experiment. An asterisk is used to denote statistical significance as determined by a one−way ANOVA with Tukey's post−hoc test. $P < 0.05$ was considered significant

Flow cytometry−myeloid cell populations

Lung cells were analyzed by flow cytometry to analyze changes in myeloid cell populations with ST3 or ST14 pneumococcal pneumonia infection. Pups infected with 1 x 10^7 CFUs *S. pneumoniae* ST14 displayed highly significant increases in granulocyte populations compared to control (Figure 19A). In fact, animals inoculated with 1 x 10^7 CFUs ST14 displayed the highest granulocyte populations compared to pups infected with 5 x 10^4 CFUs ST3 or ST14 (Figure 19A). However, there were no significant differences in mϕ populations between any of the treatment groups relative to control (Figure 19B).

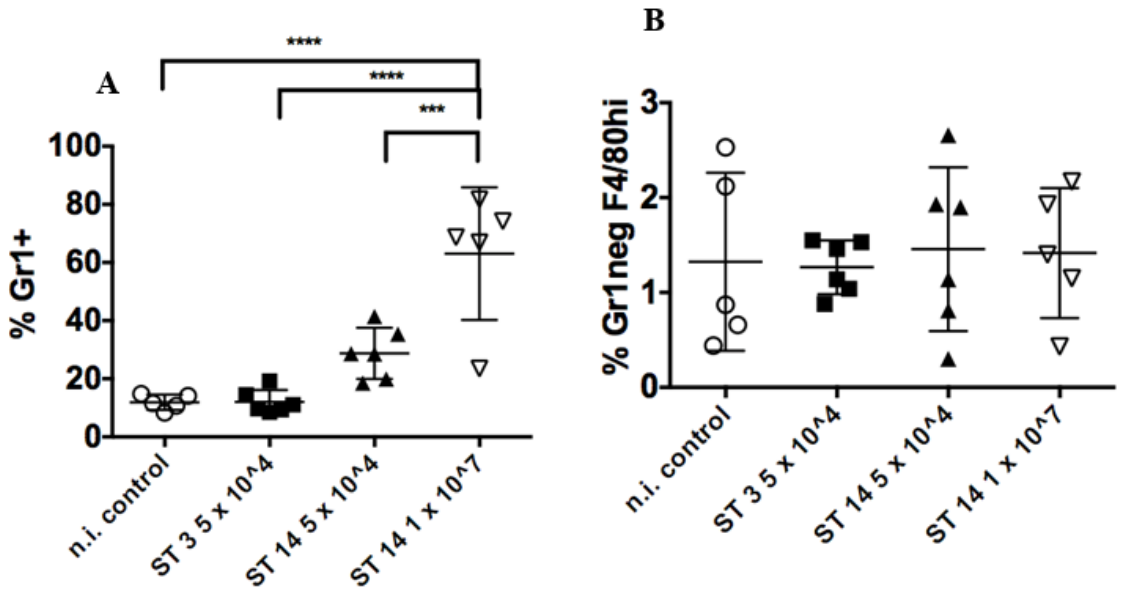

Figure 19: Myeloid cell populations at 48 h p.i.

Two x 10^5 lung cells from *S. pneumoniae* ST3− or ST14− infected animals (neonates pnd 14), were stained with 0.1 µg of Gr−1, CD11b, F4/80, and CD11c. R1 gate was chosen to include presumably live lymphocyte populations. Each plot represents a single animal from one *in vivo* experiment ± SD. Data was analyzed for significance between the serotypes by one−way ANOVA with Tukey's post−hoc test. $P < 0.05$ (denoted by a, b) was considered significant. A) CD11b+/Gr−1+ populations represent the granulocyte population. B) Within the CD11b+/Gr−1+ gate, the % of cells Gr−1−/F4/80^{Hi} represents the macrophage population.

Flow cytometry−NK cell populations

Lung cells were stained with the appropriate antibodies and analyzed for CD marker expression on a flow cytometer. The percentage of NK cells did not differ based on ST inoculation or amount of infectious dose, as determine by a one−way ANOVA with Tukey's post−hoc analysis (Figure 20A). However, the percentage of NK T cells was significantly increased in animals infected with 5 x 10^4 CFUs of ST3 relative to control (Figure 20B). The percentage of NK T cells was also higher in pups inoculated with 5 x 10^4 CFUs ST3 compared to those infected with 1 x 10^7 CFUs ST14. Please note, however, that the NK population makes up a very small percentage of lung leukocytes (Figures 20A and 20B).

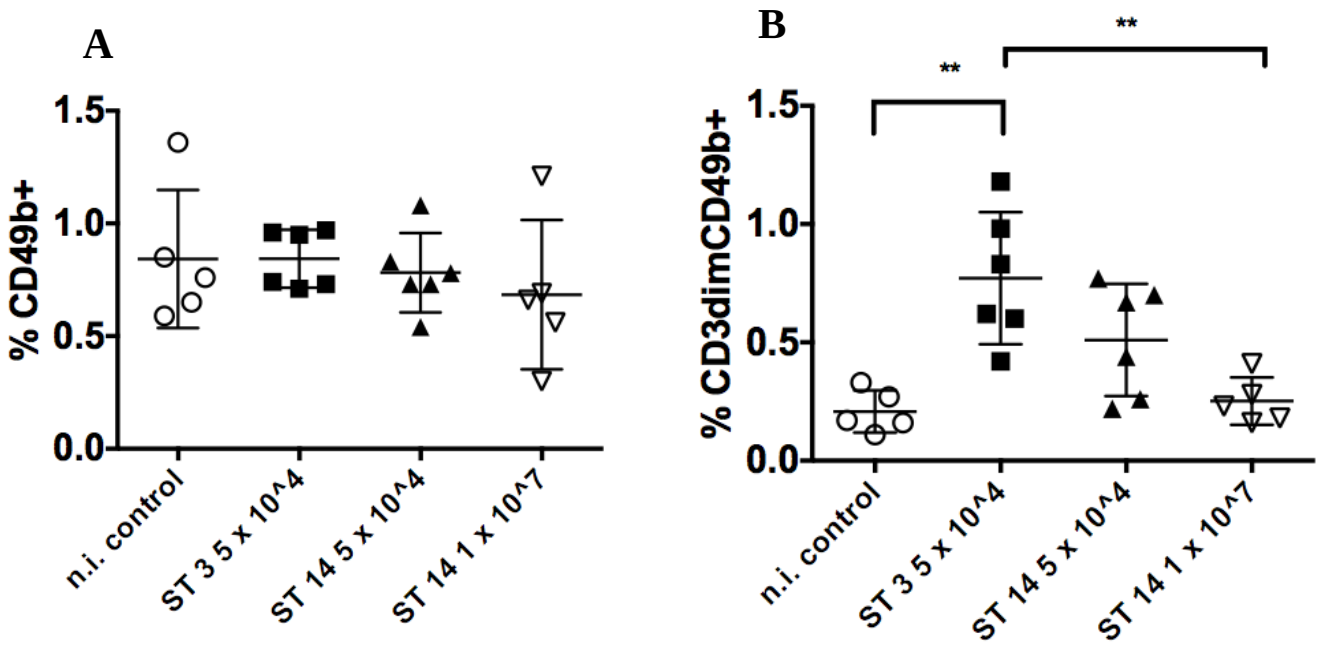

Figure 20: NK cell populations at 48 h p.i.

Two x 10^5 lung cells from *S. pneumoniae* ST3− or ST14− infected animals (neonates pnd 14), were stained with 0.1 μg of CD27, CD11b, CD49b, and CD3. R1 gate was chosen to include presumably live lymphocyte populations. Each plot represents a single animal from one *in vivo* experiment ± SD. Data was analyzed for significance between the serotypes by one−way ANOVA with Tukey's post−hoc test. $P < 0.05$ was considered significant (denoted with an asterisk). A) Within the $CD11b^{Int}$ gate, CD49b+/CD27+ populations represent the NK cell population. B) Of the % of cells CD49b+/CD27+, cells that were CD3 dim represent the NK T cell population.

Chapter 5

Discussion

RA controls a variety of complex immune functions, such as CD4+ T cell differentiation and function, leukocyte trafficking in the gut, and iTreg cell differentiation and function, all of which are crucial for normal immune homeostasis and protection from foreign invaders. However, RA cannot perform these functions if the VA status of the host is compromised. Thus, VA supplementation has been instituted in various developing countries to bolster the immune status and overall well−being of children and adults. Children greater than 6 months of age are currently supplemented with VA, but the efficacy of VA supplementation in neonates (i.e., 0−6 months of age) has not been explored (42). Neonates are born with naturally low VA levels, and are highly susceptible to infectious pathogens, such as *Streptococcus pneumoniae.* Thus, we sought to determine the efficacy of VA supplementation in neonatal mice before an acute *S. pneumoniae* upper respiratory tract infection.

In the first set of experiments, neonatal mice (pnd 12 and 13) were supplemented with 1550 μg of retinyl palmitate in 10 μl of oil one time per day for 2 days before a bolus inoculating dose of *S. pneumoniae* ST 3 or ST14 on pnd 14. We hypothesized that this bolus dose supplementation would increase the percentage of antibody−secreting plasma B cells, and attenuate the pathogenesis of an acute pneumococcal pneumonia infection. Animals were sacrificed at 4, 12, and 24 h p.i., and lungs were used to determine infiltrating immune cell populations and bacterial loads present at the site of infection. We found that VA supplementation had no effect on pathogen clearance from the lung or blood of infected mice. Additionally, VA generally did not have an effect on the immune cell populations in the lung. However, there was a significant increase in mϕ populations in the lung of neonates infected with

a high dose (1 x 10^7 CFUs) of ST3 at 4 h p.i. Conversely, the MFI of mϕ was decreased in animals infected with ST3 and supplemented with VA 12 h p.i.

Moreover, the common myeloid progenitor cell will differentiate into mature neutrophils in the presence of polarizing cytokines and RA, but an increase in granulocyte population or MFI with VA supplementation was not observed (43). However, a distinct trend between serotypes was observed. Generally, animals infected with ST14 had lower granulocyte populations compared to ST3−infected animals, but the MFI of ST14−infected animals was higher than those animals inoculated with ST3. DC populations were also analyzed in the lung of ST3− and ST14−infected mice. Surprisingly, VA had no effect on DC populations or MFI relative to animals supplemented with vehicle.

Later studies went on to characterize B and T lymphocytes in the lung. In the first experiment, B220 was used as the B cell marker. B220 is an early marker of B cells, but this marker is also present on other cell types (known as CD45R-positive cells−a marker of lymphocyte development). Thus, CD19 was used in later experiments to characterize the B cell population. CD19 is found on the surface of double−positive, single−positive, and mature B cells, and is a more accurate marker. RA is known to promote the antibody response, but we did not see increased B cell populations or enhanced pneumococcal clearance in infected animals that were supplemented with retinyl palmitate. However, there was a highly significant increase in B cell MFI (with B220 as a marker) in the control samples, but the infected animals did not display the same increase. Additionally, we observed an inverse relationship between CD19+ populations and CD19 expression (MFI). Specifically, animals infected with ST3 had a much larger CD19+ population compared to animals infected with ST14, but the MFI was greater in animals infected with ST 14 compared to ST 3. However, the increase in MFI was not considered significant as determined by Bonferroni's post−hoc analysis.

Initial studies only looked at the acute−phase response, so we attempted to extend the time points in order to better characterize the adaptive immune response. In experiment 3, animals were dosed and inoculated as in previous experiments, and were going to be sacrificed at 48 and 72 h p.i. However, the mortality was extremely high in all treatment groups, and the majority of animals were dead by 24 h p.i. The cause of this high mortality was unknown. Additionally, the majority of tissue samples could not be harvested and analyzed. With the few samples we could obtain, we did see a modest increase in NK T cell activity with VA supplementation (data not shown). Furthermore, samples stained with myeloid and lymphocyte cocktails were combined with data from the first 2 experiments.

Finally, the population of T lymphocytes was analyzed in the lung. Retinyl palmitate supplementation had no effect on the percentage of T cells in the lung or MFI, but a trend was observed between serotypes. Infection with *S. pneumoniae* ST3 increased the T cell population in the lung, but the MFI was slightly lower than those animals infected with ST14.

A myeloperoxidase assay was used to confirm the increased levels of neutrophil activity observed in the animals infected with ST14. Indeed, there was a highly significant increase in neutrophil activity at 12 h p.i in mice inoculated with ST14. Neutrophils are one of the first responders to the site of infection, and this may explain why ST14 infections are considerably less fatal than an infection with ST 3.

Liver ROH levels were assessed in the infected and control neonates, and it was discovered that their VA status was actually adequate, rather than marginal as we suspected. This may explain why VA supplementation had no effect on pneumococcal pathogenesis or leukocyte populations in the lung. Although the questions addressed in the previous experiments were highly significant, failure to make the pups VAM compromised the integrity of the experiments. Therefore, for the next set of experiments we decided to focus on ST3 and ST14 pathogenesis in neonates without analyzing the effect of diet or retinyl palmitate supplementation.

In all the previous experiments, animals were inoculated with a bolus dose of the infectious agent, but we wanted to see what effect a low dose (i.e., 1 x 10^3) would have on pneumococcal colonization and clearance. Therefore, animals were infected with a low dose of ST3 or S14 and sacrificed at 48 h p.i. To our surprise, only one pup had any colonies in the lung after overnight growth. We hypothesize that there must be a form of quorum sensing between the bacteria before they can take up residence in a host and cause disease. Moreover, granulocyte and NK/NK T cell populations in the lung were not significantly different relative to control.

Thus, we increased the infectious dose in the final experiment. However, the control mice had abnormally high granulocyte populations relative to control mice from other experiments. In previous experiments we sacrificed the control animals before inoculating the rest of the cage, but we felt we could sacrifice both control and infected mice together since *S. pneumoniae* is not an airborne pathogen. However, the environment the control mice were housed in must have influenced the immune populations in the lung, altering the statistical analysis for the experiment. Despite the abnormal controls, the high dose of ST14 caused a large granulocyte infiltration to the lung compared to the low dose of ST14 and ST3 infection. Additionally, animals infected with ST3 displayed an increase in NK T cells relative to control and animals infected with a high dose of ST14.

Based on these experiments, we can conclude that infection with ST14 causes a massive granulocyte infiltration to the lung, resulting in faster pathogen clearance in the host. However, it is not appropriate to conclude that VA has no effect on pneumococcal colonization and pathogenesis because the pups did not obtain the initial VA marginal status we had aimed for. Thus, future studies should focus on a better model of pneumococcal pneumonia in neonates. We will begin to use rats for these infection studies because they are easier to make VAM or VAD. We can then focus on elucidating the interaction between an acute pneumococcal pneumonia infection and VA supplementation in neonates. Additionally, pneumolysin concentration will be

assessed in the lung via RT−PCR. Mice infected with ST14 have abnormally swollen lungs compared to animals infected with ST3. That is, the lung of ST14−infected mice is larger, and appears more inflamed than lungs in animals infected with ST3. Thus, immunohistochemical analysis and pneumolysin concentration will be performed to analyze the presence of proinflammatory mediators and pneumolysin present in the lung, respectively.

In summary, the experiments presented in this thesis help to elucidate the pathogenic differences between an invasive and noninvasive ST of *S. pneumoniae*, and also suggest some changes to the murine pneumococcal pneumonia model for the future.

Appendix A

Summary of *in vivo* Treatment Groups

Note: extremely high mortality with experiment 3 (supplementation studies). Only body weight data could be obtained with this experiment. Flow data and CFUs are not included in results section.

VA supplementation studies Infectious dose = 1 x 10^7			
Time points (h)	Exp 1	Exp 2	Exp 3
4	X		
12	X	X	
24	X	X	X
48			X
72			X
VA suppplementation	X	X	X
ST 3 vs. ST 14 comparison studies Infectious dose = 1 x 10^3 (exp 1) ST 3 infectious dose = 5 x 10^4 (exp 2) ST 14 infectious dose = 1 x 10^7 (exp 2)			
48	X	X	

Appendix B

Flow Cytometry Antibody Details

Antibody	Known as	Conjugate fluorochrome	Provider
anti−Gr−1		FITC	BD Biosciences San Jose, CA
anti−B220	CD45 Protein tyrosine phosphatase, receptor type C	PE	Southern Biotechnology Birmingham, AL
anti−CD45	Protein tyrosine phosphatase, receptor type C	PeCy7	eBioscience San Diego, CA
anti−F4/80	EGF−like module−containing mucin−like hormone receptor like−1	APC	eBioscience San Diego, CA
anti−CD11b	Integrin alpha M	PE	BD Biosciences San Jose, CA
anti−CD3	T cell co−receptor	Alexa647	BD Biosciences San Jose, CA
anti−CD11c	Integrin alpha X (complement component 3 receptor 4 subunit)	FITC	BD Biosciences San Jose, CA
anti−CD49b	Integrin alpha subunit−one half of $\alpha 2\beta 1$ duplex	APC	eBioscience San Diego, CA
anti−CD27	Member of the TNF receptor family	PECy7	eBioscience San Diego, CA
anti−CD19	B−lymphocyte antigen CD19	PE	eBioscience, San Diego, CA

BIBLIOGRAPHY

1. **Jakobsen, H., Hannesdottir, S., Bjarnarson, S.P., Schuls, D., Trannoy, E., Siegrist, C., and Jonsdottir, I.** 2006. Early life T cell responses to pneumococcal conjugates increase with age and determine the polysaccharide−specific antibody response and protective efficacy. Eur. J. Immunol. **36**: 287−295.
2. **Kadioglu, A., Weiser, J.N., Paton, J.C., and Andrew, P.W.** 2008. The role of *Streptococcus pneumoniae* virulence factors in host respiratory colonization and disease. Nat. Rev. Microbiol. **6**: 288−301.
3. **Weiser, J.N.** 2009. The pneumococcus: why a commensal misbehaves. J. Mol. Med. **88**: 97−102.
4. **McCool, T.L., Cate, T.R., Moy, G., and Weiser, J.N.** 2002. The immune response to pneumococcal proteins during experimental human carriage. J. Exp. Med. **195**: 359−365.
5. **Musher, D.M., Montoya, R., and Wanahita, A.** 2004. Diagnostic value of microscopic examination of Gram−stained sputum and sputum cultures in patients with bacteremic pneumococcal pneumonia. Clin. Infect. Dis. **39**: 165−169.
6. **Koppe, U., Suttorp, N., and Opitz, B.** 2012. Recognition of *Streptococcus pneumoniae* by the innate immune system. Cell. Microbiol. **14**: 460−466.
7. **Malley, R.** 2010. Antibody and cell−mediated immunity to *Streptococcus pneumoniae*: implications for vaccine development. J. Mol. Med (Berl). **88**: 135−142.
8. **Van der Poll, T. and Opal, S.M.** 2009. Pathogenesis, treatment, and prevention of pneumococcal pneumonia. Lancet. **347**: 1543−1556.
9. **Weinberger, D.M., Trzcinski, K., Lu, Y., Bogaert, D., Brandes, A., Galagan, J., Anderson, P.W., Malley, R., and Lipsitch, M.** 2009. Pneumococcal capsular polysaccharide structure predicts serotype prevalence. PLoS Pathog. **5**: e1000476.
10. **Sa−Leao, R. and Tomasz, A.** 2009. *Streptococcus pneumoniae*. Bacteria. 304−317.
11. **Grabenstein, J.D. and Musey, L.K.** 2014. Differences in serious clinical outcomes of infection caused by specific pneumococcal serotypes among adults. Vaccine. **14**: in press.
12. **Safari, D., Dekker, H.A.T., Joosten, J.A.F., Michalik, D., Carvalho de Suza, A., Adamo, R., Lahmann, M., Sundgren, A., Oscarson S., Kamerling, J.P., and Snippe, H.** 2008. Identification of the smallest structure capable of evoking opsonophagocytic antibodies against *Streptococcus pneumoniae* serotype 14. Infect. Immun. **76**: 4615−4623.
13. **Ada, G and Isaacs, D.** 2003. Carbohydrate−protein conjugate vaccines. Clin. Microbiol. Infect. **9**: 79−85.
14. **Weinberger, D.M., Trzcinski, K., Lu, Y., Bogaert, D., Brandes, A., Galagan, J., Anderson, P.W., Malley, R., Lipsitch, M.** 2009. Pneumococcal polysaccharide capsule structure predicts serotype prevalence. PLoS Pathog. **5**: e1000476.
15. **McCool, T.L. and Weiser, J.N.** 2004. Limited role of antibody in clearance of *Streptococcus pneumoniae* in a murine model of colonization. Infect. Immun. **72**: 5807−5813.

16. **Henriques−Normark, B. and Normark, S.** 2010. Commensal pathogens, with a focus on *Streptococcus pneumoniae*, and interactions with the human host. Exp. Cell. Res. **316**: 1408−1414.
17. **Reynolds, H.Y.** 1998. Host defense mechanisms in the respiratory tract, p. 364 *In* Stein, J.H. (ed.), Internal Medicine, 5th ed. Mosby Inc, St. Louis.
18. **Ammann, A.J.** 1981. Immunology of *Streptococcus pneumoniae*, p.25 *In* Nahmias, A.J. and O'Reily (eds.), Immunology of Human Infections, Vol 8, Pt. 2. Plenum Medical Book Co., New York.
19. **Lammers, A.J., de Porto, A.P., de Boer, O.J., Florquin, S., and Van der Poll, T.** 2012. The role of TLR2 in the host response to pneumococcal pneumonia in absence of the spleen. BMC Infect. Dis. **12**: 139−157.
20. **Blaschke, A.J.** 2011. Interpreting assays for the detection of *Streptococcus pneumoniae*. Clin. Infect. Dis. **52**(suppl_4): S331−S337.
21. **Jensen, K.M., Melchjorsen, J., Dagnaes−Hansen, F., Sorensen, U., Laursen, R.R., Ostergaard, L., Sogaard, O.S., and Tolstrup, M.** 2012. Timing of toll−like receptor 9 agonist administration in pneumococcal vaccination impacts both humoral and cellular immune responses as well as nasopharyngeal colonization in mice. Infect. Immun. **80**: 1744−1752.
22. **Bogaert, D., de Groot, R., and Hermans, P.W.M.** 2004. *Streptococcus pneumoniae* colonisation: the key to pneumococcal disease. Lancet Infect. Dis. **4**: 144−154.
23. **Ross, A.C., Chen, Q., and Ma, Y.** 2011. Vitamin A and retinoic acid in the regulation of B−cell development and antibody production, p. 103 *In* Litwack, G. (ed.), Vitamins and Hormones, Vol 86. Academic Press, Burlington.
24. **Lee, C. and Lee, L.H.** 2005. Mucosal immunity induced by pneumococcal glycoconjugate. Crit. Rev. Microbiol. **31**: 137−144.
25. **Malley, R., Trzcinski, K., Srivastava, A., Thompson, C.M., Anderson, P.W., and Lipsitch, M.** 2005. $CD4^+$ T cells mediate antibody−independent acquired immunity to pneumococcal colonization. Proc. Natl. Acad. Sci. USA. **102**: 4848−4853.
26. **Lipsitch M., Whitney, C.G., Zell, E., Kaijalainen, T., Dagan, R., and Malley, R.** 2005. Age-specific incidence of invasive pneumococcal disease by serotype: are anticapsular antibodies the primary mechanism of protection against invasive disease? PLOS Med. **2**:e15.
27. **Alicino, C., Barberis, I., Orsi, A., and Durando, P.** 2014. Pneumococcal vaccination strategies in adult population: perspectives with the pneumococcal 13−valent polysaccharide conjugate vaccine. Minerva Med. **105**: 89−97.
28. **Pauksens, K., Nilsson, A.C., Caubet, M., Pascal, T.G., Van Belle, P., Poolman, J.T., Vandepapelière, P.G., Verlant, V., and Vink, P.E.** 2014. Randomized controlled study of pneumococcal vaccine formulations contains PhtD and dPly proteins with alum or adjuvant system AS02V in elderly adults: safety and immunogenicity. Clin. Vaccine Immunol. [Epub ahead of print].
29. **Ross, A.C. and Harrison, E.H.** 2007. Vitamin A: Nutritional Aspects of Retinoids and Carotenoids *In* Zempleni, J., Rucker, R.B., McCormick, D.B., and Suttie, J.W. (eds.), Handbook of Vitamins, 4th edition. Taylor and Francis Group, LLC., Boca Raton.
30. **D'Ambrosio, D.N., Clugston, R.D., and Blaner, W.S.** 2011. Vitamin A metabolism: an update. Nutrients. **3**: 63−103.

31. **Schreiber, R., Taschler, U., Preiss−Landl, K., Wongsiriroj, N., Zimmermann, R., and Lass, A.** 2012. Retinyl ester hydrolases and their roles in vitamin A homeostasis. Biochim. Biophys. Acta. **1821**: 113−123.
32. **Pino−Lagos, K., Benson, M.J., and Noelle, R.J.** 2008. Retinoic acid in the immune system. Ann. N.Y. Acad. Sci. **1143**: 170−187.
33. **Hall, J.A., Grainger, J.R., Spencer, S.P., and Belkaid, Y.** 2011. The role of retinoic acid in tolerance and immunity. **35**: 13−22.
34. **Iwata, M., Hirakiyama, A., Eshima, Y., Kagechika, H., Kato, C., and Song, S.Y.** 2004. Retinoic acid imprints gut−homing specificity on T cells. Immunity. **21**: 527−538.
35. **Snoeck, V., Peters, I., Cox, E**. 2006. The IgA system: a comparison of structure and function in different species. Vet. Res. **37**: 455–467.
36. **Mora, J.R., Iwata, M., Eksteen, B., Song, S.Y., Junt, T., Senman, B., Otipoby, K.L., Yokota, A., Takeuchi, H., Ricciardi−Castagnoli, P., Rajewsky, K., Adams, D.H., and von Andrian, U.H.** 2006. Generation of gut−homing IgA−secreting B cells by intestinal dendritic cells. Science. **314**: 1157−1160.
37. **Ross, A.C.** 2012. Vitamin A and retinoic acid in T cell−related immunity. Am. J. Clin. Nutr. **96**: 1166S−1172S.
38. **Kimura, A. and Kishimoto, T**. 2010. IL-6: regulator of Treg/Th17 balance. Eur. J. Immunol. **40**:1830–1835.
39. **Xiao, S., Jin, H., Korn, T., Liu, S.M., Oukka, M., Lim, B., and Kuchroo, V.K**. 2008. Retinoic acid increases Foxp3+ regulatory T cells and inhibits development of Th17 cells by enhancing TGF-beta-driven Smad3 signaling and inhibiting IL-6 and IL23 receptor expression. J. Immunol. **181**: 2277–2284.
40. **Mills, K.H.G.** 2004. Regulatory T cells: friend or foe in immunity to infection?. Nat. Rev. Immunol. **4**: 841−855.
41. **National Institute of Allergy and Infectious Disease.** 2014. Pneumococcal Disease. <http://www.niaid.nih.gov/topics/pneumococal/pages/pneumococcaldisease.aspx>
42. **World Health Orgnization.** 2014. Micronutrient Deficiencies−Vitamin A Deficiency. <http://www.who.int/nutrition/topics/vad/en/>
43. **Gupta, D., Shah, H.P., Malu, K., Berliner, N., and Gaines, P.** 2014. Differentiation and characterization of myeloid cells. Curr. Protoc. Immunol. **104**: 22F.5.1−22F.5.28.

Tiffany M. Bernardo Academic Vita

317 E. Beaver Avenue • State College, PA 16801
Phone: (724)-681-1343 • E-Mail: tbernardo1234@gmail.com

EDUCATION

The Pennsylvania State University, **Schreyer Honors College**

- Bachelor of Science Candidate
- Minor in Microbiology, emphasis in Biochemistry
- Undergraduate Honors Thesis: A Comparison of *Streptococcus pneumoniae* Serotype 3 and Serotype 14 Infection in Neonatal Mice
- Graduation date: May 2014

PROFESSIONAL EXPERIENCE

Undergraduate Honors Research, 2012−present
Department of Nutritional Sciences, The Pennsylvania State University
Research advisor: Dr. A. Catharine Ross

- Retinoids/Immunology Laboratory
- Investigation of vitamin A status on immune cell infiltration and pathogen colonization during invasive *Streptococcus pneumoniae* infection in neonatal mice
- Proficient in: Ultra Performance Liquid Chromatography (UPLC), RNA isolation, RT-PCR, Q-PCR, quantitative plate counts, ELISA, dissection and tissue collection in adult and neonatal mice, facial vein bleeds, and flow cytometry prep/analysis

HONORS AND AWARDS

- Academic competitiveness grant (university−wide scholarship), 2009−2011
- Kochanowski-Poirier Trustee Scholarship, 2011−2012
- Tewksbury Trustee Scholarship, 2012−2013
- Schreyer Honors Special Project Grant, spring 2013
- Fasola Family Trustee Scholarship, 2013−2014
- Lord Academic Excel Scholarship, 2013−2014

ASSOCIATION MEMBERSHIPS

Schreyer Honors College – The Pennsylvania State University
May 2012 - present
Golden Key Honor Society
September 2011 – present
National Society of Collegiate Scholars
August 2011 – present
College of Health and Human Development Honor Society
Spring 2011 – present

ACTIVITIES

Heal House/Impact THON
-Penn State IFC/Panhellenic Dance Marathon for childhood cancer
-Member of the canning committee that plans fundraising weekends